CHAPTER 4

Solid-phase reactors

4.1 Introduction

The introduction of solid-phase reactors in flow systems represents a high achievement for on-line determination of different substances [1,2]. The development of the system in flow injection analysis (FIA) and lately in sequential injection analysis (SIA) has revolutionalised flow systems.

There are various types of solid-phase reactors which have been developed. The type dictates the purpose for which it is intended. The solid-phase reactors developed to date are enzymatic, immuno-assay, ion-exchange, redox, absorbent extractors or reagent releasers. In all these the concept of immobilization still leads.

The use of reagents, particularly enzymes in the solid-phase has been known from the early part of the 20th century. These enzymes where immobilized on a variety of support materials for a number of reasons [3].

The use of these immobilized reagents thus offered a greater degree of control over the relevant reactions. These type of heterogeneous reactions have been converted for use in FIA with some success [4,5]. In addition to the excellent analytical features already available with the incorporation of solid-phase reactors in FIA, further advantages with respect to miniaturization, sample reduction, efficiency and cost reduction can be expected from SIA.

Different types of immobilization techniques for solid-phase reactors are described in this Chapter, along with the shapes and designs of reactors used, the location of the reactor in the system manifold in both FIA and SIA are given. The various applications are also given for both FIA and SIA.

The FIA methodology using a solid-phase reactor has advanced remarkably and its adaptation to SIA is already gaining momentum and is expected to enhance and improve this technique to such an extent that almost any analyte can be determined, especially with regard to the most expensive, slightly soluble and insoluble ones.

4.2 Reactor types and preparation

The approach in the preparation of solid-phase reactors is dictated by its nature and the analytical purpose of its immobilization. There are various ways in which these reactors can be designed and hence, the name for each reactor is related to the type of material it is made of. Solid-phase reactors can be classified into two distinct groups, namely reactors in which a chemical reaction takes place to derivatise the analyte and reactors in which no derivatising reaction takes place. The first group includes, among others, enzyme reactors while the second group consists mostly of reactors used for pre-concentration.

4.2.1 Derivatising reactors

4.2.1.1 Redox reactors

Redox reactors are prepared by packing the micro or mini columns with redox material. The material may be dry or a slurry of the reagent. When immobilized, it is allowed to be trapped while the polymer is forming and hardening to form oxidizing beds. This type of reactor employs a string of oxidizing (e.g. MnO_2 or PbO_2) [6,7] or reducing agent [5,8,9], which reacts with the analyte of importance to either render it in a suitable oxidation state for further reaction or for direct detection. The driving force for this type of reactor is the reduction or oxidation potential of the immobilized reagent. For the determination of nitrate the cadmium metal acted as a reductor in the following equation:

$$Cd\ (s) + NO_3\ (aq) + H_2O\ (\ell) \rightleftharpoons Cd^{2+}\ (aq) + NO^-_2\ (aq) + 2\ OH^-\ (aq)\ ;\quad E_0 = 6.402\ V$$

Redox reactors are also used to prepare analytes for enzyme immobilization.

4.2.1.2 Complex-forming reactors

The complex formation reactors are prepared by packing the column with a finely divided reagent. In this case the complexing agent, or ligand, is immobilized and reacts selectively with the metal analyte of importance when the latter moves through the reactor [10]. A typical

reaction that may be used is:

$$Fe^{3+}(aq) + Tiron^{2-}(s) \Leftrightarrow [Fe(Tiron)]^{+}(aq)$$

In this case the tiron (1,2 - dihydroxybenzene- 3, 5 - disulphonate) is in the reactor and reacts when the iron passes through. This reaction takes place in acidic medium. The resulting complex can be detected spectrophotometrically at the wavelength of maximum absorption. This reactor works on the premises that the formation constant of the complex is high enough to overcome the interactive forces between the ligand and the support material, whether it be ionic or polar-polar interaction.

4.2.1.3 Precipitating reactors

This type of reactor is ideally suited for the indirect determination of anions. A very slightly soluble compound is immobilized in the reactor and reacts with the analyte to form an even less soluble compound, releasing more soluble ion into the carrier stream [11]. This ion should then be in an easily detectable state, for example chromate or dichromate whose absorbance is measured directly. A typical reaction that takes place is the following:

$$BaCrO_4(s) + SO_4^{2-}(aq) \rightarrow BaSO_4(s) + CrO_4^{2-}(aq)$$

The solubility product of the analyte with different counter-ions plays an important role in developing a method incorporating this type of reactor. In this case the solubility product for $BaCrO_4$ ($K_{sp} = 2.4 \times 10^{-10}$) is higher than that for $BaSO_4$ ($K_{sp} = 1.1 \times 10^{-10}$) and the latter would

thus precipitate, releasing the chromate into the carrier stream. The sulphate content of a sample can be indirectly determined in this fashion [11].

4.2.1.4 Enzyme reactors

Enzymes are extremely efficient biological catalysts that can increase the rate of some occasionally very complex chemical reactors by a few orders of magnitude. Many reactors would be analytically useless in the absence of enzymes. Enzyme reactors are prepared by enzymes immobilized on suitable supports; particularly controlled-pore glass (CPG). The CPG provides support of readily available particle size, pore diameter and specific surface area. Silica excel over organic polymers.

Technology for enzyme catalysed reactions for use in flow systems is also quite well known and these reactors comprise most of the solid-phase reactors currently in use [4,5,12,13]. The specificity of enzyme reactors ensure that there are few, if any, interferences for a given method and thus also reduce the enzyme consumption, which is an important factor when the high cost of enzymes are considered.

A reaction consisting of four steps for the determination of inosine in human blood plasma is given below as an example of the simplicity and specificity possible with immobilized enzyme reactors in flow injection systems. The reaction that takes place is the following:

$$\text{Inosine} \xrightarrow{PNP} \text{hypoxanthine} \xrightarrow{XOD} \text{xanthine} \xrightarrow{XOD} \text{uric acid} \xrightarrow{UOD} \text{alantoin}$$

where PNP = purine nudeoside phosphorylase

XOD = xanthine oxidase

and UOD = urate oxidase

In the last three steps of the above reaction hydrogen peroxide is evolved, which then reacts with K - (P-hydroxyphenyl) propionic acid (HPPA) in a horseradish peroxidase (HRP) mediated step to form a fluorosphore compound which can be detected fluorimetrically [4]. A diagram of the FIA system is given in Fig. 4.1 which can easily be adapted to an SIA system as postvalve location.

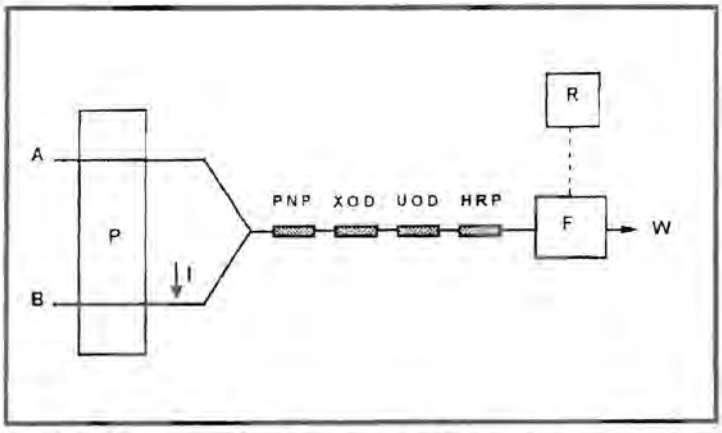

Fig. 4.1 Enzyme catalysed reaction in a flow system

In Fig. 4.1, **A** = HPPA; **P** = Peristaltic pump; **I** = Point of sample injection; **F** = Fluorescence detector; **R** = Recorder and **W** = Waste.

4.2.1.5 Immunoassay

The application of flow injection analysis (FIA) to immunology offers promise of faster and

more reproducible assays. It was found to be advantageous in that it is possible to utilize the kinetics of immunochemical binding. It uses immobilized reactors which binds the species of interest while allowing the rest of the matrix to pass through the reactor.

The bead injection (BI) is introduced as a novel flow system especially for immunoassay. The BI can be traced back to early literature of FIA. It was however, the SI technique that made it possible to handle suspended beads with precision and reliability. The introduction of BI resulted in an improvement to the SI system where in-line regeneration drawbacks were avoided. Other advantages of BI include improved assay sensitivity, because the use of surface bounded reagents minimizes sample dilution, lower limits of detection (because the analyte can accumulate on the beads) [14]. The detection method typically involves a tag such as an enzyme, radioisotope or fluoropore to monitor the reaction with a variety of detectors.

4.2.2 Non-derivatising reactors

4.2.2.1 Adsorptive reactors

The most commonly used material for packing adsorptive reactors is C18 bonded silica beads and to a lesser extent alumina and silica. Other packing material such as polyurethane foam (PUF) on a mini column are also used. Pre-concentration of metal ions is the most important use for this type of reactor, which consist of an adsorptive material like resins used for HPLC, packed in a conical container with both ends plugged with porous material.

Pre-concentration in a conical shape reactor takes place from the narrow to the wider end in a

conduit, with elution taking place in the opposite direction. The elution of the analyte through a narrow aperture introduces a well-defined sample zone into the carrier stream.

The adsorptive reactor may be used as a flow through sensor for individual as well as multi-element determination [15,16]. These reactors are based on the principle that the adsorptive material is placed in the flow cell of a flow system (FIA/SIA) and retains a product formed in the system for absorbance or reflectance measuring. Multi-element determination was done with the aid of a diode array spectrophotometer.

4.2.2.2 Reagent releaser reactors

Reagent releaser reactors are prepared by packing the reagents in cartridges or bound to resins. These reactors have as their aim the decrease in dispersion of a sample plug by eliminating the merging point in a flow system usually necessary for reagent addition. The reagent is thus added from the solid-phase directly into the sample, where it will release the relevant reagents into the carrier stream. The system is also simplified, as the merging points in the case of more than one reagent usually requires teflon connectors and extra tubing.

4.2.2.3 Beads

Bead injection (BI) is a technique based on the microfluidic manipulation of a precise volume of suspended sepharose beads that serve as a solid-phase carrier for reagents or reactive groups. It is composed of 80% solution and 20% matrix and are highly transparent to light. BI combines the advantages of solid-phase chemistry with the novelty of fluidic handling of microcarrier

beads, allowing automated surface renewal and postanalysis manipulations [116]

4.3 Modes of immobilization

There are three basic types of immobilization, namely natural, physical and chemical.

4.3.1 Natural

This type of immobilization is used when the reagent is naturally very slightly soluble in the relevant medium and the particles are of approximately the desired size and consistency [17]. Large particles can also be ground to the desired size if necessary [11]. Usually one would want the particles as small as possible to have the maximum surface area available for reaction, but this may provide problems as the basic-pressure resulting from usage of such small particles proves too much for normal peristaltic pumps to handle. This type of pump is mostly used in FIA to keep the total Piston-type pumps which can handle higher pressure, but this elevates the total cost. The Gilson mini pulse peristaltic pump is used in SIA. A compromise should be reached between the maximum surface area available with small particles and effective back-pressure produced in the system.

4.3.2 Adsorption

This type of immobilization, is mostly used when the reagent is a polar or even an ionic species [18]. The support for the polar reagent is a corresponding polar compound such as silica or

alumina and for the ionic species, a suitable ionic compound, such as an ion-exchange resin. The reagent is adsorbed onto the polar material either by precipitation, or heating and evaporation of the solvent. Other packing material such as polyurethane foam (PUF) on a mini column are also used. Pre-concentration and separation is the most commonly used function for this reactors.

In Chapters 5 and 8 the adsorption of lead (IV) dioxide onto silica gel is described for use in a redox reactor. There the immobilization was achieved by oxidising an aqueous lead(II) solution with sodium hypochlorite, whereafter a solid precipitate was formed. The precipitate (PbO_2) immediately adsorbed onto the very polar silica gel present in the reaction mixture.

4.3.3 Entrapment

This method is often used for enzyme immobilization when doing pharmaceutical analyses [6,7]. It involves making a slurry of the reagent to be immobilized, and physically "trapping" or encapsulating it in a hardening polymer. Polyester resins are particularly useful in this regard. Martinez Calatayud and Garcia Mateo [7] described the use of a polyester resin to immobilize Copper (II) carbonate. A copper(II) carbonate slurry was stirred together with AL-100-A polyester resin and a small volume of the relevant catalyst added. This mixture was then stirred until it started to harden. The resin with entrapped reagent ($CuCO_3$) could then be ground to the desired size and introduced into a reactor. This method for the immobilization of solid reagents provides a great degree of control over the amount of immobilizes reagent as well as the reagent to support ratio.

4.4 Shape of the reactor/ Reactor design

There are different reactor shapes that are used in FIA but now also in SIA. The shape that the reactor assumes, is indicative of whether a chemical reaction needs to take place or not.

4.4.1 Tubular

The most common reactors used are tubular or cylindrical in shape because of the flow through nature of the method. The reagent, either immobilized on a support material or naturally insoluble, can be packed into the tube, column or cylinder with both ends of the reactor closed off by glass wool or a similar porous inert material. Fig. 4.2 shows a cylindrical reactor that is used in Chapters 6 and 7, while Fig. 4.3 shows a packed tubular reactor used in Chapters 5 and 8.

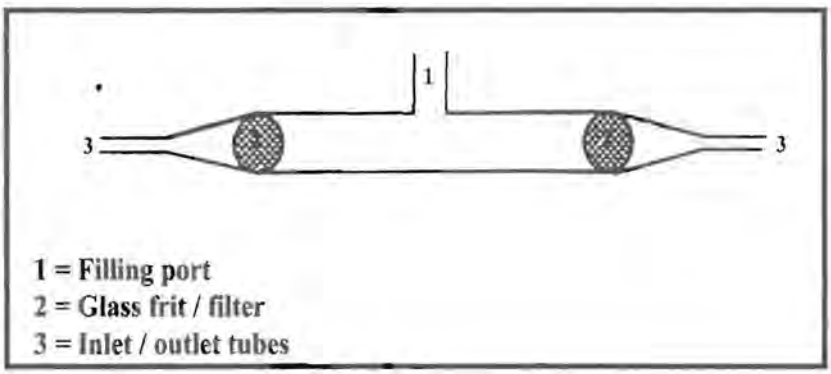

Fig. 4.2 Design of a cylindrical reactor

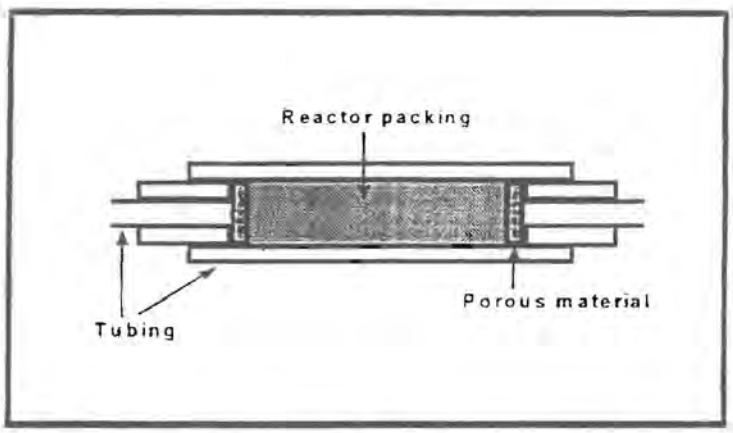

Fig. 4.3 Design of a packed tubular reactor

A open tubular reactor where the reagent is absorbed or impregnated on or in the tube wall is shown in Fig. 4.4. This reactor is less resistant to flow and the activity of its layers is rather low, so very long tubes are required to allow the reaction to proceed to the point at which detection becomes possible.

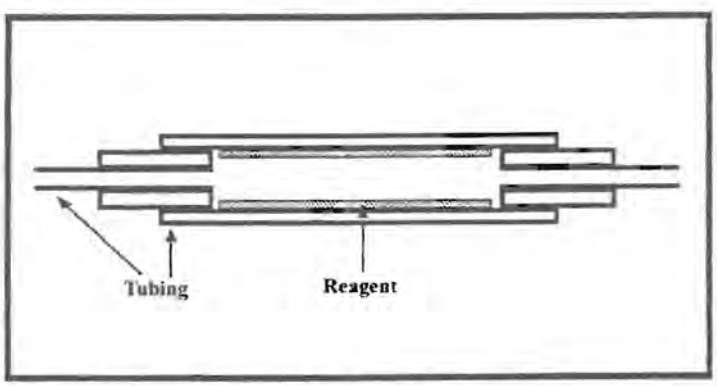

Fig. 4.4 Design of an open tubular reactor

4.4.2 Conical

A typical design of a push-fit conical reactor is shown in Fig. 4.5. The conical reactor is used when constructing pre-concentration reactors and enrichment factors of up to 50 have been achieved with it [19].

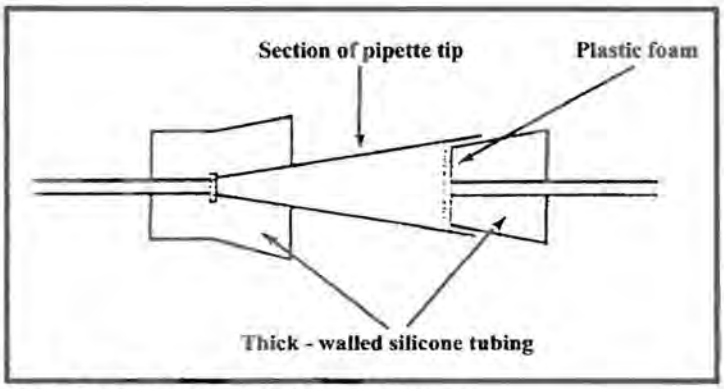

Fig. 4.5 Design of a push-fit conical reactor

The conical shape of a pre-concentration reactor ensures minimum dispersion of the retained analyte on elution, because retention takes place from the narrow to the wider end, while elution takes place in the opposite direction (Thus, elution of the analyte through a narrow aperture introduces a well-defined sample zone into the carrier stream).

A reactor with threaded fitting is shown in Fig. 4.6. This type of reactor can be constructed with push-fit or threaded fittings for coupling to the transmission tubing, with each type of fitting having its own advantages and disadvantages with regard to ease of construction and long term reliability. Reactors with threaded fittings are preferred over push-fit reactors

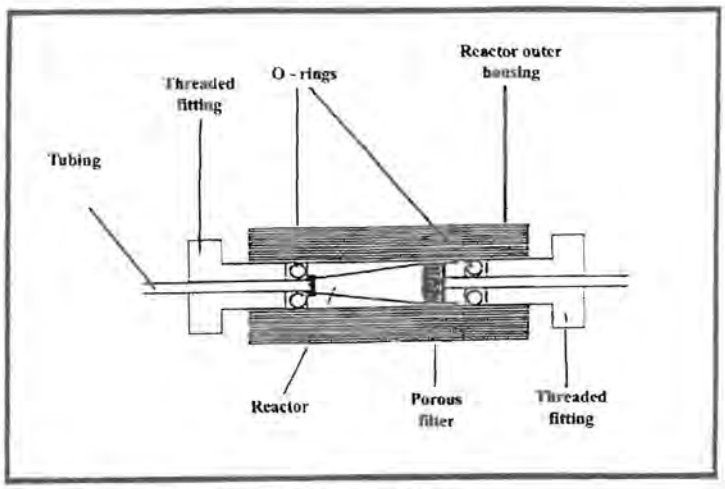

Fig. 4.6 Conical reactor with threaded fittings

4.4.3 Jet ring cell /Beads

Solid-phase titration is a novel technique that uses beads as individual micro-vessels containing a titrant and an indicator [20]. Beads injection (BI) is a novel approach to assays based on liquid-solid interactions.

The technique is based on the micro-fluidic manipulation of a precise volume of suspended beads that serve as a solid-phase carrier for reagents or reactive groups. Fig. 4.7 shows an SI system diagram modified for BI.

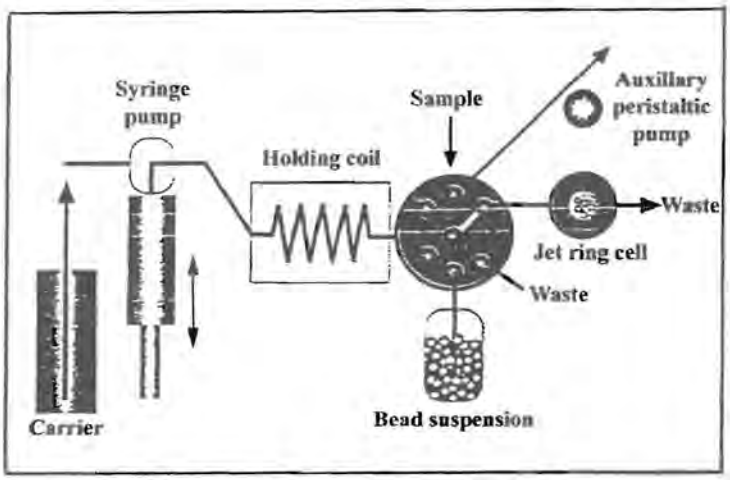

Fig. 4.7 An SIA diagram with beads and a jet ring cell

The use of beads as reagent carrier is restricted to biology, biotechnology and drug discovery in which there is an immediate need for kinetic interaction assays.

4.5 Position of reactor in the system

Reactors can be placed in many different positions along the FIA/SIA manifold depending on their analytical purpose. Illustration for both FIA and SIA system will be given in some cases for clarity.

4.5.1 Pre-valve position for the reactor

Fig. 4.8 and 4.9 show the position of the reactor in the FIA and SIA manifolds respectively.

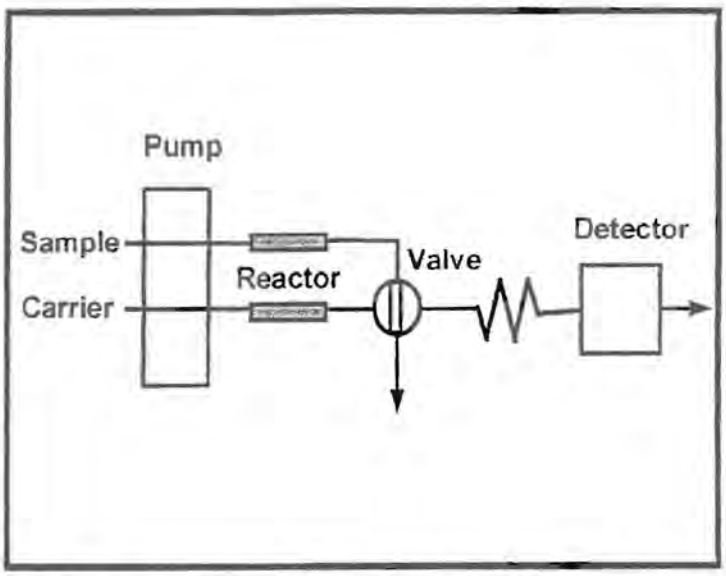

Fig. 4.8 Prevalve position for the reactor in a FIA system

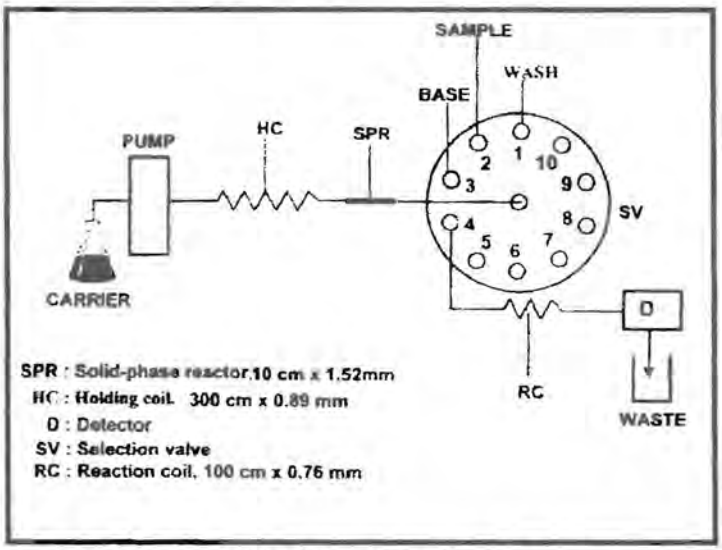

Fig. 4.9 Prevalve position for a reactor in a SIA system

This location is employed when there are impurities in either the carrier or sample stream and the aim is to minimize or remove the impurities. The reactor in this case is usually an adsorptive reactor packed with G8 bonded silica for the removal of less polar components or to a lesser extent, silica or alumina for the removal of more polar compounds. It may also be a redox material where the sample must first be reduced or oxidised before it can react, or combine with any reagent or before it can be propelled to the detector.

4.5.2 Between the injection valve and detector

Any type of reactor can be used in this location for any application, whether it be enzymatic, catalytic, redox, pre-concentration or complexation. The reactor in this case may act as sample converter or reagent releaser.

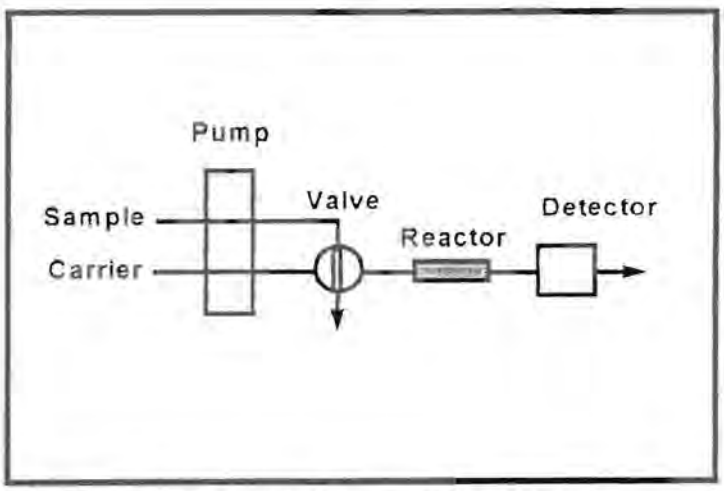

Fig. 4.10 Post-valve position for a reactor in a FIA system

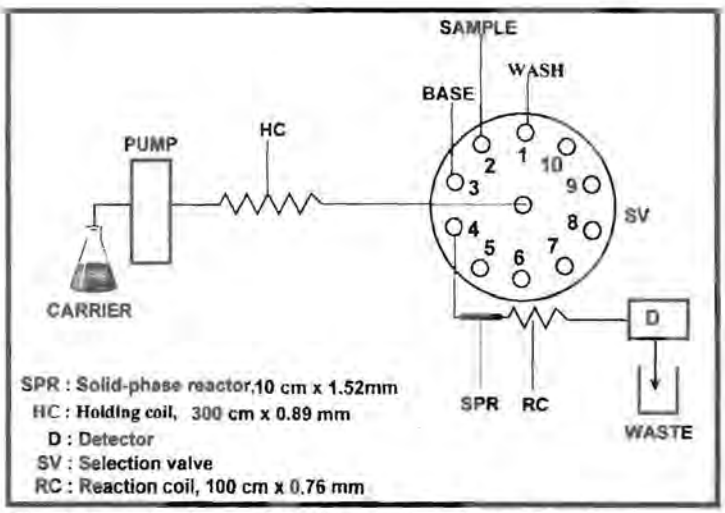

Fig. 4.11 Post-valve position for a reactor in a SIA system

4.5.3 In the injection system

This location is mostly used for pre-concentration with an adsorptive reactor placed in the sample loop of the injection system [21]. The released analyte can then be eluted with a suitable eluent and pumped to the detector. A schematic diagram of this arrangement applicable only to FIA is in Fig. 4.12. However, in the case of SIA, the same pre-concentration technique may be used, but instead, the adsorptive reactor is placed before the selection valve as in Fig. 4.9 where preconcentration can take place. The released analyte is then be eluted with a suitable eluent and pumped to the detector.

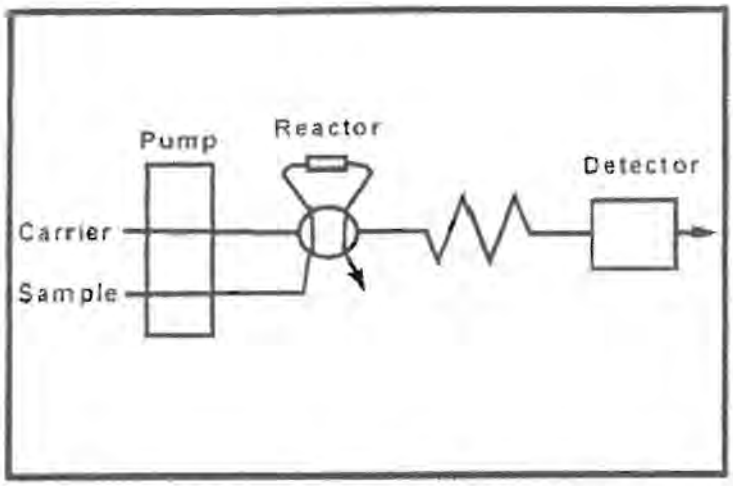

Fig. 4.12 Diagram of reactor placed in the injection system in a FIA manifold

4.5.4 In the detector

This location for the reactor is used to integrate reaction and detection for a number of advantages, some of which are decreased dispersion of the sample zone, increased sensitivity and increased sample throughput. The system can be extremely small. And there is no need for an additional reaction unit or transport tubing because the reactor is in the detector system. Diagrams of this arrangement are shown in Figures 4.13 and 4.14 for FIA and SIA systems respectively.

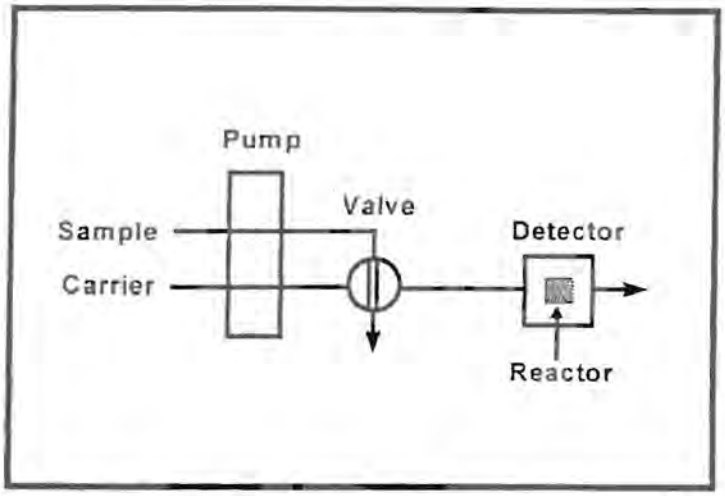

Fig. 4.13 Diagram of a FIA system with detector in the detection unit

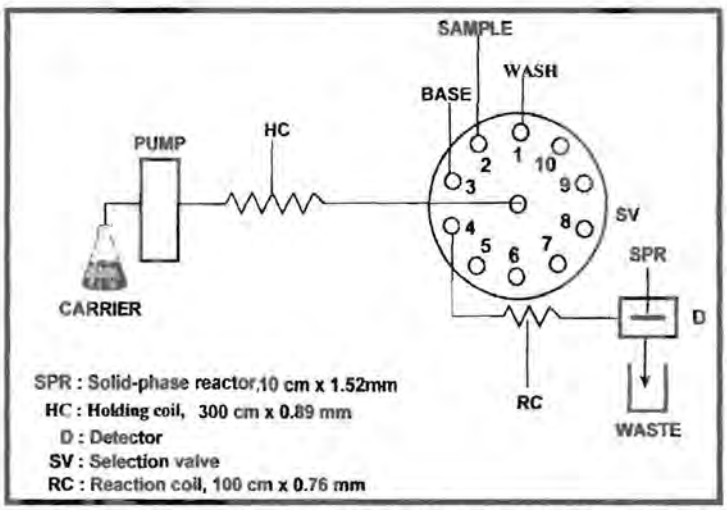

Fig. 4.14 Diagram of a SIA system with detector in the detection unit

4.6 Application of solid-phase reactors

To discuss the application of solid-phase reactors, the applications involved in FIA will be the starting point. A brief discussion of the reagent releaser will be given first followed by an analytical performance and reactor type given in Tabular form. This section will end with a brief discussion on SIA application.

4.6.1 FIA solid-phase reactors

Reagent releasers are very useful means of increasing sensitivity through substantially decreased dilution. A flow-through optosensor [116] in conjuction with a mono-channel FIA with fluorimetric detection, using sephadex SP-25 resin as active sorbent substrate was used for determination of vitamin B6 (pyridoxine).

Table 4.1 gives the analytical performance, the reactor and detector type for adsorptive reactors while Table 4. 2 shows the substances analysed and the performance of each detector type for ion-exchange reactors.

TABLE 4.1. Substances analysed using solid-phase adsorptive reactors in FIA.

Analyte	Range	%RSD	Detector	Ref
Pt	0.1 - 5 µg/ℓ	7 - 9	FAAS	23
Citrate, isocitrate	0.25 - 5 mmol/ℓ	2	Amperometry	24
Cr(III), Cr		1.2 - 5.9,1.2 - 5.7	FAAS	25
Pt	0 - 250 mg/ℓ	4.0	ICP-MS	26
Pt	20 - 80 µg/ℓ		ICP-AES	27
Co, Cu	0.3 - 6 µg/mℓ 0.1 - 15 µg/mℓ	2, 0.9	Spectrometrry	28
Cd, Pb	0.02 - 0.2 µg/ℓ	2.1 - 2.7	ETAAS	29
Cr			ETAAS	30
Zn	20 - 100 ng/ℓ	1.2	Spectrometry	31
Urea	0 - 120 mg/ℓ	< 1,9	Spectrometry	32
Hg	0 - 1 µg/mℓ	0.8 - 2.1	ICP-AES	33
V, Pb, Co, Cd			Spectrometry	34
Zn	0.04 - 40 ng/ℓ	3.3	Spectrometry	35
Ni	0.25 - 5 µg/ℓ	1.1	Spectrometry	36
Aspartame	20 - 80 µg/mℓ	0.2	Chemilumetry	37
Al	0.3 - 16 µmol/ℓ	3.7	Specrometry	38
Ag	0 - 800 ng/ℓ	1	Amperometry	39

TABLE 4.2 Substances analysed using Ion-exchange as solid phase reactor in FIA

Analyte	Range	%RSD	Detector	Ref
Trace metals			ETAAS	40
Chloracetic acid	0.005 - 0.1 mol/ℓ	1.5	Potentiometry	41
Pb		2.4	FAAS	42
Cd	0.056 - 56.2 mg/ℓ	7	Potentiometry	43
Cd			Potentiometry	44
Anion surfactants	0.005 - 0.5 mmol/ℓ	0.7	Phosphorescence	45
L- valine, L-leucine, L - isoleucine	30 nmol/ℓ - 5 µmol/ℓ	1.6	Potentiometry	46
Am, Pu			α- spectroscopy	47
Fe (total)	1 - 50 mg/ℓ	1.1	Spectrometry	48
Cu	0 - 100 µg/ℓ	< 2	Spectrometry	49
Se	100 - 200 ng/ℓ	1.5 - 2.3	ETAAS	50
Trace metals			AAS	51
Trace metals		3 - 5	ICP-MS/AAS	52
Trans-resveratrol	0 - 100 mg/ℓ	3.2 - 7.1	Spectrometry	53
Ascorbic acid	1.0 - 6.0 µg/mℓ	0.87 - 1.08	Spectrometry	54

Redox reactors develop a strong reducing or oxidizing agent which reacts with the analyte of importance to either render in a suitable oxidation state for further reaction or for direct detection. Redox reactors are also used to prepare analytes for enzyme immobilization. Table 4.3 gives the substances determined and the performance of the reactor and detector.

TABLE 4.3. Substances analysed using solid phase redox reactor in FIA.

Analyte	Range	%RSD	Detector	Ref
Adrenaline	0.5 - 20 µg/mℓ	2.0	Fluorimetry	55
Emetine hydrochloride	0.1 - 100 µg/mℓ	1.3	Fluorimetry	56
Phenothiazine derivatives	5 - 50 µg/mℓ	0.5 - 1.0	Spectrometry	57
Mn	0 - 5 mg/ℓ	1.8	Spectrometry	10
L -ascorbic acid	50 - 400 µmol/ℓ	0.75	Spectrometry	58
Sulfide	1.0 - 5.0 µg/ℓ	2.3	Spectrometry	59
Cystein	1 - 90 µg/mℓ	0.8	Spectrometry	60
Thioradazine, chlorpromazine	250 - 500 µg/mℓ	3.4 , 2.8	Spectrometry	61
Iproniazid, isoniazid	0 - 14 µg/mℓ	1.4	Spectrometry	62
H_2O_2	0.01 - 0.1 mol/ℓ		Spectrometry	63
Phenothiazine derivatives	5 - 150 g/mℓ	1.2	Potentiometry	64
Chlorpromazine	0.1 - 2 µg/mℓ	1.4	Potentiometry	65
Nitrate, Nitrite	0.02 - 400 µg/ℓ	1.56, 0.77	Spectrometry	9
Mn	1- 20 mg/ℓ	1.35	Spectrometriy	66

The use of immobilized enzymes in FIA emerges from a simple to a complex one. Many reactors would be analytically useless in the absence of enzymes. This is shown in Table 4.4 by the long list of various substances analysed and the performance of the chosen detector and reactor.

TABLE 4.4. Substances analysed using immoblized enzymes in FIA.

Analyte	Range	%RSD	Detector	Ref
Starch			Spectrometry	67
Ammonia. Glutamine			Potentiometry	68
Nitrophenyl phosphates	0 - 0.16 µmol/ℓ			69
Creatine, glucose , urea	0.2 - 20 mmol/ℓ		Electrochemical	70
Phosohate, pyrophosphate		1.5	Amperometric	71
Glycogen				72
Glutamic acid	10 - 500 µmol/ℓ	1.8	Spectrometry	73
Creatine, creatinine	5 - 400 µmol/ℓ	0.7	Spectrometry	74
Glucose uric acid, cholesterol			Amperometry	75
Nucleotides, Purine	0 - 10 µmol/ℓ	2.2 - 3.8	Amperometry	76
Creatinine			Amperometry	77
Methanol	4 - 80 µmol/ℓ	1.8	Fluorimetry	78
Glucose, glutamate, acetylcholine			Amperometry	79
Glucose, uric acid, cholesterol	5 - 700 mg/ℓ	2.8	Amperometry	80
Glucose,butyrate-3-hydroxy	10 µmol/ℓ - 1 mmol/ℓ 1 µmol/ℓ - 0.5 mmol/ℓ	0.88 1.1	Chemiluminescence	81
Glucose, penicillin			Spectrometry	82
L - Malic acid	20- 400 µmol/ℓ	1.2	Amperometry	83
Glycerol				84
Nitrogen containing compounds	0.005 - 8 mmol/ℓ	2	Fluorimetry	85
KI	0.06 - 100 µmol/ℓ		Chemiluminescence	86
Glutamate	0.05 - 20 mmol/ℓ	1.9 - 2.8	Spectrometry	87

Glycerol, ATP	2 -160 µmol/ℓ, 4 70 µmol/ℓ		Spectrometry	88
Lysine , glucose			Chemiluminescence	89
Glucose, choline	30 n mol/ℓ - 10µmol/ℓ	2	Chemiluminescence	90
Review			Chemiluminescence	91
Creatine, urea	0.05 - 1.5 mmol/ℓ	0.9 - 1.2	Spectrometry	92
Catechol, dopamine, phenol			Spectrometry	93
Biosystems			Ammonium-ion sensor	94
α-glycerophosphate			Spectrometry	95
inosine, hypoxanthine	0 - 20 µmol/ℓ	2.3	Amperometry	96
H_2O_2	40 - 80 mol/ℓ	1.1	Fluorimetry	97
ATP, ADP, AMP	2.5 - 2500 pmol 10 - 2500 pmol 25 - 5000 pmol	3.5 2.0 2.2	Fibre-optic sensor	98
Serine, sucrose	0 - 0.5 g/ℓ, 0 - 2.5 g/ℓ	1.7, 0.75	Amperometry	99
β - N - oxalyl, α,β - diamino propionic acid			Amperometry	100
Formaldehyde	0.5 - 100 µg/ℓ	0.92	Amperometric	101
D and L- amino acids			Amperometry	102
Glutamate	1 - 200 µmol/ℓ, 10 - 500 µmol/ℓ		Fluorimetry	103
Branched chain amino acids			Fluorimetry	104
NADP	0.01 - 5 µmol/ℓ	1.5 - 2.3	Fluorimetry	105

The application of FIA to immunology has resulted in a method which offers promise for faster and more reproducible assays. FIA was found to be advantageous in that it is possible to utilize the kinetics of immunochemical binding. Table 5 gives the various substances analysed and the

performance of the chosen reactor and detector.

TABLE 4.5. Substances analysed using immunochemical binding in FIA

Analyte	Range	%RSD	Detector	Ref
Immunoglobulin			Fluorimetry	106
Insulin	0.05 -2.25 ng/mℓ	4	Fluorimetry	107
Cr, imazethepyr	10 - 200 ng/mℓ		Fluorimetry	108
Biomolecules			Immunoassay	109
Bioligands			Spectrometry	110
Choline , phospholipidase	0.2 -1 ng/mℓ	1.8	Chemiluminescence	111
Eschericia, enterotoxin, staphylococcal			Fluorimetry	112
Pesticides			Immunoassay	113
microcarrier beads			beads	114
Drugs			Fluorimetry	2, 115
Atrazine	0.014 - 0.232 ng/mℓ		Fluorimetry	116
Naptalam		3.7	Fluorimetry	117

4.6.2 SIA solid-phase reactors

The use of solid-phase reactors incorporated into the SIA manifold is one of the areas which still needs a lot of exploration as little has been done compared to FIA. However, focus is now put on SIA. Shu *et al.* [118] developed a spectrophotometric method for the determination of lactic acid from industrial inorganics. A method for the simultaneous monitoring of glucose, lactic acid and penicillin [119] by SIA with glucose oxidase or lactate oxidase immobilized onto nylon

tubing was developed. The on-line monitoring of glucose and penicillin [120] with immobilized glucose oxidase and penicillinase on a piece of nylon tubing from industrial organics was accomplished spectrophotometrically.

Theophylline and caffeine [121] using a micro-column packed with Micro-prep High Q anion exchange beads were determined spectrophotometrically. The separation of radio-nuclides [122] using Sr-resin, TRU-resin and TEVA resin beads as slurry packed into a micro-column was developed.

4.7 Conclusion

FIA methodology using solid-phase has advanced to a very large extent that almost any analyte can be determined. The substances analysed ranges from agricultural, industrial, environmental, clinical, bioassay and biochemical (Tables 4.1 - 4.5). The number of publications in international journals and the journal for FIA is further evidence of the interest it has generated.

The simplicity and versatility of this technique allows the location of the solid reactor in the manifold in accordance to the nature of the analysis desired. The adaptation of the FIA technique to SIA has started to emanate, this is evident from the number of publications gradually coming out.

The same reactor types and shapes used in FIA are used in SIA. The only difference is with the location of the reactor in the manifold, with SIA needing fewer positions to execute the same

function.

Although the on-line coupling of solid-phase reactors to both the FIA and SIA manifold are related to one of the these three aspects, namely: miniaturization, integration of reaction (retention) and detection as well as multianalyte determinations, the SIA technique has enhanced sensitivity and is more cost effective. Thus SIA with solid-phase reactor incorporated into its manifold is a trend which has to be looked into.

4.8 References

1. M. D. Luque de Castro, **Trends Anal. Chem., 11** (1992) 149.
2. J. Martinez and J. V. Garcia Mateo, **Trends Anal. Chem., 12** (993) 428.
3. R. A. Messing, **Immobilised enzymes for industrial reactors, Academic Press,** New York,1975.
4. K. Zaitsu, K. Yamagashi and Y. Okhura, **Chem. Pharm. Bull., 36** (1988) 4488
5. Y. Hayashi, K. Zaitsu and Y. Okhura, **Anal. Chim. Acta, 186** (1986) 131.
6. J. Martinez-Catalayud, J. V. Garcia Mateo and Lahuerta Zamora, **Anal. Chim. Acta, 265** (1992) 81.
7. J. Martinez-Catalayud and J. V. Garcia Mateo, **Anal. Chim. Acta, 274** (1993) 275.
8. T. Pérez-Ruiz, C. Martinez-Lozano, V. Tomás and J. Carpena, **Analyst (London), 117** (1992) 1025.
9. J. F. van Staden and Makhapa Makhafola, **S. Afr. J. Chem., 52(1)** (1999) 49.
10. J. F. van Staden and L. G. Kluever, **Anal. Chim. Acta, 350** (1197) 15.
11. A. Sakuragawa, S. Nakayama and T. Okutani, **Anal. Sci., 10** (1994) 77.
12. A. Fernandez, J. Ruz, M. D. Luque de Castro and M . Valcárcel, **Clin. Chim. Acta, 148** (1985) 131.
13. C. W. Bradberry and R. N. Adams, **Anal. Chem., 55** (1983) 2439.
14. J. Růžička and L. Scampavia, **Anal. Chem. News and Features,** (1999) 251A.
15. D. Chen, M. D. Luque de Castro and M. Valcárcel, **Microchem. J., 44** (1991) 215.
16. B. Fernández-Band, F. Lazaro, M. D. Luque de Castro and M. Valcárcel, **Anal. Chim. Acta, 229** (1990) 177.

17. R. Montero, M. Gallego and M. Valcárcel, **Anal. Chim. Acta, 234** (1990) 433.

18. J. Martinez-Calatayud and S. Sagrado Vivez, **J. Pharm. Anal., 7** (1989) 1165.

19. Z. Fang, **Flow-Injection Separation and Preconcentration**, VCH, Weinheim, 1993.

20. D. H. Holman, G. D. Christian and J. Růžička, **Anal. Chem., 69** (1997) 1763.

21. M. Karlson, J. C. Person and J. Möller, **Anal. Chim. Acta, 244** (1991) 109.

22. A. Ruiz-Medina, M. L. Fernandez-de-Cordova and A. Molina-Diaz, **Fresenius' J. Anal. Chem., 363** (1999) 265.

23. A. Cantarero, M. M. Gomez, C. C. Camara and M. A. Palacios, **Anal. Chim. Acta, 296** (1994) 205.

24. K. Matsomoto and T. Tsukatani, **Anal. Chim. Acta, 321** (1996) 157.

25. R. M. Cespon-Romeo, M. C. Yebra-Biurrun and M. P. Bernejo-Barrera, **Anal. Chim. Acta, 327** (1996) 37.

26. M. M. Hidalgo, M. M. Gomez and M. A. Palacios, **Fresenius' J. Anal. Chem., 354** (1996)420.

27. J. F. van Staden, C. J. Rademeyer and S. M. Linsky, **S.Afr. J. Chem., 50** (1997) 115.

28. E. Vereda, A. Rios and M. Valcarcel, **Analyst 122** (1997) 85.

29. E. Ivanova, W. Van Mol and F. Adams, **Spectrochimica Acta, Part B53** (1998) 1041.

30. S. Nielsen and E. H. Hansen, **Anal. Chim. Acta, 366** (1998)163.

31. D. S. de Jesus, R. J. Cassella, S. L. C. Ferreira, A. C. S. Costa, M. S. de Carvalho, R. E. Santelli, **Anal. Chim. Acta, 366** (1998) 263.

32. S. Jorgi, D. Narinesingh and T T. Ngo, **Anal. Lett., 31** (1998) 543.

33. P. Canada-Rudner, J. M. Cano-Pavon, F. Sanchez-Rojas and A. Garcia-de-Torres, **J. Anal. At. Spectron, 13** (1998) 1167.

34. D. Beauchemin and A. A. Spech, **Canadian J. Anal. Sci. And Spectrosc., 43** (1998) 43.

35. S. G. L. Teixeira, F. R. P. Rocha, M. Korn, B. F. Reis, S. G. L .C. Ferreira, A. C. S. Costa, **Anal. Chim. Acta, 383** (1999) 309.

36. S. L. C. Ferreira, D. S. de Jesus, R. J. Cassella, A. C. S. Costa, M. S. de Carvallo and R. E. Santelli, **Anal. Chim. Acta, 378** (1999) 287.

37. O. Fatibello-Filho, L. H. Marcolino-Junior and A. V. Pereira, **Anal. Chim. Acta, 384** (1999) 167.

38. K. J. Powel, **Analyst, 123** (1998) 797.

39. Q. S. Pu, Q. Y. Sun, Z . D . HU and Z. X. Su, **Analyst, 123** (1998) 239.

40. P. E. Carreiro J. F. Tyson, **Analyst, 122** (1997) 95.

41. C. Puig-Lleixa, J. Bartroli, M. Del-valle, D. Montllo and A. Tomico, **Anal. Chim. Acta, 359** (1998) 311.

42. G. H. Tao and Z. L. Fang, **Fresenius' J. Anal. Chem., 366** (1998) 156.

43. C. M . C .M. Couto, J. L. F .C. Lima, B. S. M. Montenegro, B. F. Reis and E. A. G. Zagatto, **Anal. Chim. Acta, 366** (1998) 155.

44. M. Trojanowicz, P. W. Alexander and D. B. Hibbert, **Anal. Chim. Acta, 370** (1998) 267.

45. R. Badia, M. E. Diaz-Garcia, **Anal. Chim. Acta, 371** (1998) 73.

46. N. Kiba, M. Tachibana, K. Tani and T. Miwa, **Anal. Chim. Acta, 375** (1998) 65.

47. J. W. Grate and O. B. Egorov, **Anal.Chem., 70** (1998) 3929.

48. J. F. van Staden and L. G. Kluever, Fresenius. **J. Anal. Chem., 362** (1998) 319.

49. F.C. Carmago, E.A.G. Zagato and C.C. Oliveira, **Anal. Sci., 14** (1998) 565.

50. P. E. Carreiro, J. F. Tyson, **Spectrochimica Acta, B53** (1998) 1931.

50. P. E. Carreiro, J. F. Tyson, **Spectrochim. Acta, B53** (1998) 1931.

51. G. M Greenway, S. M. Nelms, I. K. Skhosana and S. J. L. Dolman, **Spectrochim. Acta, Part B 51 B** (1996) 1909.

52. S. N. Willie, H. Tekgul and R.E. Sturgeon, **Talanta, 47** (1998) 439.

53. L. Arce, M. I. Tena, A. Rios and M. Valcarcel, **Anal. Chim. Acta, 359** (1998) 27.

54. A. Molina-Diaz, A. Ruiz-Medina and M. L. Fernandez de Cordova, **Fresenius J. Anal. Chem., 363** (1999) 92.

55. A. Kojlo and J. M. Calatayud, **Anal. Lett., 28** (1995) 239.

56. S. L . Ortiz and J. Martinez Calatayud, **Anal. Lett., 28** (1995) 971.

57. A. Kojlo and J. M. Calatayud, **Talanta, 42** (1995) 909..

58. A. V. Pereira, O. Fatibello-Flho, **Anal. Chim. Acta, 366** (1998) 55.

59. J. F. van Staden and L. G. Kluever, **Anal. Chim. Acta, 369** (1998) 157.

60. M. Catala-Icardo, L. Lahuerta-Zamora and J. Martinez Calatayud, **Analyst, 123** (1998) 1685.

61. M. Catala-Icardo, L. Lahuerta-Zamora and J. Martinez-Calatayud, **Lab. Robotics. Autom. 10** (1998) 33.

62. J. A. Garcia-Bautista, J. V. Garcia-Mateo and J. Martinez-Calatayud, **Anal. Lett., 31** (1998) 1209.

63. J. A. Garcia-Bautista, J. V. Garcia-Mateo, J. Martinez-Calatayud, **J. Flow. Injection. Anal., 15** (1998) 61.

64. M. Polasek, J. Dolejsova and R. Karlicek, **Pharmazie, 53** (1998) 168.

65. A. Kojlo, **Anal. Lett., 30** (1999) 2353..

66. K. Kargosha and M. Noroozifar, **Anal. Chim. Acta, 413** (2000) 57.

67. J. Emneus, G. Nilson and L. Gorton, **Starch/Staerke, 45** (1993) 264.

68. B. O. Palson, B. Q. Shen, M. E. Meyerhoff and M. Trojanowicz, **Analyst, 118** (1993) 1361.

69. Y. Shan, I. D. Mckelvie and B. T. Hart, **Anal. Chim., 65** (1993) 3053.

70. C. S. Rui, H. I. Ogawa, K. Sonomoto and Y. K ato, **Biosci. Biotechnol.Biochem, 57** (1993) 191.

71. T. Yao, and T. Wasa, **Electroanalysis (NY), 5** (1993) 887.

72. J. Emneus and L. Gorton, **Anal. Chim. Acta, 276** (1993) 319.

73. C. D. Stalikas, M. I. Karayannis, S. M. Tzouwara-Karayanni, **Analyst, 118** (1993) 723.

74. G. Moges and G. Johansson, **Anal. Lett., 27** (1994) 495.

75. T. Yao, M. Satomura and T. Nakahara, **Anal. Chim. Acta, 296** (1994) 271.

76. T. Yao, K. Tsureyaman and T. Nakahara, **Electroanalysis (NY), 6** (1994) 165.

77. C. S. Rui, Y. Kato and K. Sonomoto, **Biosens-Bioelectron, 9** (1994) 429.

78. C. G. de Maria, T. Manzano, R. Duarte, A. Alfonso, **Anal. Chim. Acta, 309** (1995) 241

79. T. Yao, S. Suzuki, H. Nishino and T. Nakahara, **Electroanalysis (NY), 7** (1995) 1114

80. .T. Yao, M. Satomura and T. Nakahara, **Electroanalysis (NY), 7** (1995) 143.

81. N. Kiba, H. Koemado and M. Furusuwa, **Anal. Sci., 11** (1995) 605.

82. R. W. Min, J. Nielsen and J. Villadsen, **Anal. Chim. Acta, 320** (1996) 199.

83. M. I. Prodrommidis, S. M. Tzouwara-Karayannis, P. Vadigamaand and A. Maines, **Analyst,121** (1996) 435.

84. M. I. Prodrommidis, C. D. Stalikas, S. M. Tzouwara-Karayannis, **Talanta, 43** (1996) 27.

85. H. Mana and U. Spohn, **Anal. Chim. Acta, 325** (1996) 93.

86. K. Hayash, T. Okugawa, Y. Kozuka, S. Sasaki, K. Ikebukuro and I. Karube, **Anal. Lett.,**

29 (1996) 2499.

87. R. Shi and K. Stein, **Analyst , 121** (1996) 1305.

88. E. R. Kiranas, M. I. Karayannis and S. M. Tzouwara-Karayanni, **Anal. Lett., 30** (1997) 537.

89. A. M. Almuaibed and A. Townshend, **Anal. Chim. Acta, 338** (1997) 149.

90. M. Emteborg (b.Stigband), K. Irgum, C. Gooijer, U. A.T. Brinkman, **Anal. Chim. Acta, 357** (1997) 111.

91. N. Kiba, **J. Flow. Injection-Anal., 14** (1997) 123.

92. M. Jurkiewicz, S. Alegret, J. Admirall, M. Garkia and Fabregas, **Analyst,123** (1998) 1321.

93. A. W. O. Lima, E. K. Vidsiunas, V. B. Nascimento and L. Angnes, **Analyst , 123** (1998) 2377.

94. M. Jurkiewicz, S. Alegret and E. Fabregas, **Anal. Chim. Acta, 370** (1998) 47.

95. E. R. Kiranas, M. I. Karayannis and S.M. Tzouwara-Karayanni, **Talanta, 45** (1998) 1015.

96. M. A. Carsol and M. Mascini, **Talanta, 47** (1998) 335.

97. Y. Z. Li and A. Townshend, **Anal. Chim. Acta, 359** (1998) 149.

98. P. E. Michel, S. M. Gautier-Sauvigne and L. J. Blum, **Anal.Chim. Acta, 360** (1998) 89.

99. P. Sosnitza, F. Irtel, R. Ulber, M. Busse, R. Faure, L. Fischer and T. Scheper, **Biosensor and Bioelectronics, 13** (1998) 1251.

100. G. Akalu, G. Johansson and B. M. Nair, **Food Chemistry, 62** (1998) 233.

101. N. Kiba, L. Sun, S. Yokose, M. T. Kazue, T.T. Suzuki, **Anal. Chim. Acta, 378** (1999) 169.

102. M. Varadi, N. Adanyi, E. E. Szabo and N. Trummer, **Biosensor and Bioelectronics, 14**

(1999) 335.

103. C. D. Stalikas, M. I. Karayannis and S. M. Tzouwara-Karayanni, **Egypt. J. Chem., 3** (1994)113.

104. N. Kiba, M. Tachibana, K. Tani and T. Miwa, **Anal. Chim. Acta, 375** (1998) 65.

105. T. Yao, H. Ogawa and T. Nakahara, **Talanta, 42** (1995) 1297.

106. C. H. Pollema and J. Ruzicka, **Anal. Chem., 66** (1994) 1825.

107. M.Y. Khokhar, J. N. Miller and N. J. Seare, **Anal. Chim. Acta, 290** (1994) 154.

108. J. Růžička, **Anal. Chim. Acta, 308** (1995) 14.

109. B.Willumsen, G. D. Christiaan and J.Růžička, **Anal. Chem., 69** (1997) 3482.

110. J. Růžička and A. Ivaska, **Anal. Chem., 69** (1997) 5024.

111. M. G. Yaqoob, J. A. Nabi and M. Masoon-Yasinzai, **J. Biolumin. Chemilumin., 12** (1997)135.

112. H. Yu, **Anal. Chim. Acta, 376** (1998) 77.

113. Z. L. Zhi, **Lab. Robotics. Autom., 11** (1999) 83.

114. J. Růžička and L. Scampavia, **Anal. Chem., 71** (1999) 257A.

115. P. S. Hodder and J. Růžička **Anal. Chem., 71** (1999) 1160.

116. M.A. Gonzalez-Martinez, R. Puchades, A. Maquieira, I. Ferrer, M. P. Marco and D. Barcelo, **Anal. Chim. Acta, 386** (1999) 201.

117. T. Galeano-Diaz, M.I. Aledo-Valenzuela and F. Saliaas, **Anal. Chim. Acta, 384** (1999) 185.

118. H. C. Shu, H. Hakanson and B. Mattiason, **Anal. Chim. Acta, 300** (1995) 277.

119. R. W. Min, J. Nielsen and J. Villadsen, **Anal. Chim. Acta, 312** (1995) 149.

120. R. W. Min, J. Nielsen and J. Villadsen, **Anal. Chim. Acta, 320** (1996) 199.

121. B. Dockendorf, D. A. Holman, G. D. Christian and J. Růžička, **Anal. Comm., 35** (1998) 357

122. O. B. Egorov, M. J. Ohara, and J. W. Grate, **Anal. Chem., 71** (1999) 345.

CHAPTER 5

Determination of manganese using a solid-phase reactor in an SIA system

5.1 Introduction

Manganese is a grey metal with a reddish tone. It is relatively abundant, constituting about 0.085% of the earth's crust. Among the heavy metals only iron is more abundant, heavier than manganese, harder and have a higher melting point (mp; Mn = 1244°C, Fe = 1535°C). Although widely distributed, it occurs in a number of substantial deposits mainly as oxides, the most important of which is pyrolusite, manganese (II) oxide, MnO_2 , is a grey-green to dark green powder made by roasting the carbonate in hydrogen or nitrogen by action of steam on manganese (II) chloride, $MnCl_2$ at 600°C. Less important ores are: braunite, Mn_2O_3 ; manganite, $Mn_2O_3.H_2O$ and hausmanite, $MnO.Mn_2O_3$. Manganese is also present in a fairly abundant impurity in most iron ores and hydrous oxide carbonate deposits [1,2]. Its presence in ground water and natural waters is considered to be due to the chemical erosion of the earth's crust [3].

Manganese exhibits complex behaviours in natural water systems, cycling readily among oxidation states in response to changing environmental conditions [4,5]. The behaviour of manganese in seasonably anoxic hypolimnetic waters generally follows the model developed by Delfino and Lee [6], who traced the migration of the boundary between oxidized and reduced forms from below the sediment-water interface up into the water column as anoxia developed

during stratification. Manganese thus resembles iron in its response to changing redox conditions, and the bio-geochemistries of the two elements are closely linked [7].

The concentration of manganese found in natural water is generally quite low, in the range 0.1-1.0 mg/ℓ [8], although in certain reservoirs at times it is as high as 10 mg/ℓ [9]. However, in South Africa the mining industry also contributes to the presence of manganese in natural waters and the concentrations may rise to a level of 200 mg /ℓ even higher in certain effluent streams [8].

Although manganese in ground water is generally present in the soluble divalent ionic form because of the absence of oxygen, part or all of the manganese in water treatment plants may be in a higher valence state. There is however, evidence that manganese occurs in surface waters both in suspension in the quadrivalent and trivalent state in a relatively stable, soluble complex.

Special means of removal such as chemical precipitation and pH adjustment, aeration and use of special ion-exchange materials has been used. Hence, the determination of manganese in public and industrial waters is important because it can cause discolouration of products, stains to laundry and reduction of pipeline carrying capacities due to encrustation. Furthermore the effect of its deficiency in both plants and animals cause diseases. Manganese at elevated concentration is toxic to a variety of organisms.

5.2 Properties of Manganese

Manganese is roughly similar to iron in its physical and chemical properties, the main difference being that it is harder and more brittle, but less refractory. It is quite electropositive and readily dissolves in dilute, non-oxidizing acids. It is not particularly reactive towards non-metals at room temperatures, but at elevated temperatures it reacts vigorously. It burns in chlorine gas to give $MnCl_2$, reacts with fluorine to give MnF_2 and MnF_3, burns in nitrogen above 1200°C to give Mn_3N_2 and combines with oxygen giving Mn_3O_4 at high temperatures. It also combines directly with boron, carbon, sulfur, silicon and phosphorus, but not with hydrogen. In neutral or acid solutions it exists as the very pale pink hexa-aquo ion, $[Mn(H_2O)_6]^{2+}$, which is quite resistant to oxidation. In basic media, however, the hydroxide, $Mn(OH)_2$ is formed and this is readily oxidized even by air [1,10]

5.3 Oxidation states of Manganese

As with Ti, V and Cr, the highest oxidation state of manganese corresponds to the total number of 3d and 4s electrons. This +7 state occurs only in the oxo compounds, MnO_4^-, Mn_2O_7 and MnO_3F, and these compounds show some similarity to corresponding compounds of the halogens. Manganese (VII) is a powerful oxidizing ion, usually being reduced to Mn(II). The intermediate oxidation states are known, but only a few compounds of Mn(V) have been characterized; nevertheless, Mn(V) species are frequently postulated as intermediates in the reduction of per-manganates. Although Mn(II) is the most stable state, it is quite readily oxidized in alkaline solution. Thus the only compounds that appear in stable ionic species in

solution are in the +2 as Mn(II) and the +7 as MnO_4^- [1,4,11].

5.4 Manganese (II) compounds: Mn^{2+}

Since the divalent state is the most important and most stable state in solution and the analyses is in water, only compounds in this oxidation state will be discussed. Manganese(II) is found in both solid salts and their aqueous solutions. In solution this ion is only slightly hydrolysed and its hydroxide is among the more soluble and more strongly basic of the precipitable hydroxides. In atmospheric oxygen the gelatinous white solid, rapidly darkens because of oxidation. It is a well defined compound, having the same crystal structure as magnesium hydroxide [1,2].

Manganese (II) forms as intensive series of salts with all common anions. Most are soluble in water, although the phosphate and carbonates are slightly so. The soluble salts of manganese include the chloride, $MnCl_2 \cdot 4H_2O$; sulphate, $MnSO_4 \cdot 4H_2O$ and nitrate, $Mn(NO_3)_2 \cdot 6H_2O$. All of these are red solids, but at a concentration greater than 0.5 mol/ℓ in water they assume a pink colour [1,10].

Manganese(II) sulfide, MnS has a pink colour and precipitates when sulfide ions in basic solution are added, and has a relatively large K_{sp} value (1×10^{-14}) and hence dissolves easily in 6 mol/ℓ HCl. Manganese(II) hydroxide, $Mn(OH)_2$ forms a pink precipitate when a solution containing Mn^{2+} is made basic. Its K_{sp} value is large enough (4×10^{-14}). The compound $Mn(OH)_2$ does not form stable complexes with either of these two species [1,2,10].

The majority of manganese(II) complexes are of a high spin. In octahedral fields, this configuration gives spin-forbidden as well as parity forbidden transitions, thus accounting for the extremely pink colour of such compounds. In tetrahedral environments, these transitions are therefore twice stronger and the compounds have a noticeable pale yellow-green colour.

Manganese(II) forms many complexes, but with the equilibrium constants for their formation in aqueous solution are not high compared to those for the divalent cations of succeeding elements [Fe(II)-Cu(II)], because the Mn(II) ion is the largest of these and it also has no ligand field stabilization energy in its complexes. Many hydrated salts contain $[Mn(H_2O)_6]^{2+}$ ion, and direct action of ammonia anhydrous salts leads to the formation of ammoniates, $[Mn(NH_3)_6]^{2+}$ ion. Chelating ligands such as ethylenediamine form $[Mn(OH)_2EDTA]^{2-}$. Hydrated salts such as trans-$[MnCl_2(H_2O)_2]^{2-}$ and trans-$[MnCl_6(H_2O)_4]^{2-}$ are also known.

5.5 Industrial uses of Manganese

Metallic manganese, as such is not used to any appreciable extent in industry. But the iron-manganese alloy called ferromanganese, which contains 75 to 80% manganese, is largely used in the manufacture of special steels. These steels are used to make rails, safe and many types of machinery.

The addition of small quantities of ferromanganese improves the quality of steel by removing traces of oxygen and sulfur on forming MnO_2 and MnS which are separated by slag. The addition of larger quantities of ferromanganese forms steel of great toughness. MnO_2 is used as

a dryer for paints since it catalyses the oxidation (drying) of the paint oils by oxygen of the air; as a decolouriser of glass, since it oxidises any green iron (II) compound present to a much paler yellow iron (III) compound; and as a depolariser in dry cells, since it reacts with the H_2 liberated at the carbon cathode. Potassium permanganate, $KMnO_4$, find some use as a strong oxidant, especially in analytical procedures [10].

5.6 Biological importance of Manganese

The biological role of manganese has stimulated much study of especially complexes of Mn(II) and Mn(VII) oxidation states. Manganese is an essential element in several biological systems in trace amounts, virtually to all forms of life. Manganese is involved in the oxidation of water to oxygen in the photo-system II where redox changes are linked to the four-electron oxidation of water. It is the only metal that has been found to be associated with the water-splitting apparatus in all the oxygen-evolving organisms studied to date [13]. In plants the bacterial enzyme super-oxide dismutase [1,2] catalyses the decomposition of O_2^-. The precise nature and role of manganese in this, is not clear and nothing is known about the chemical details of its participation [14]. Nevertheless searches for model systems have led to study polydentate [15] and macro-cyclic ligands [16] such as polyamine carboxylate, 8- quinolinolates, polyhydroxo compounds and porphyrins.

Although manganese is an essential element in plant and animals, at elevated concentrations are toxic to a variety of aquatic organism [13]. In addition, reduced manganese makes water unpalatable and causes fouling and corrosion in water systems and cooling towers. Deficiencies

cause diseases of both plants and animals in larger numbers. The adult human body contains approximately 15 mg of manganese.

In the quality of water for human consumption the maximum admissible concentration is 0.05 mg/ℓ and the guide value is 0.02 mg/ℓ; the WHO and European Standards quotes 0.05 mg/ℓ as the level above which trouble may arise; the Russian Standards allow 0.1 mg/ℓ as the upper limit; earlier surface water criteria in the United States suggested a similar value of 0.05 mg/ℓ [17]. If manganese precipitates out in water as manganese (II) hydroxide in a distribution system so that the consumers receive a blackened discolouration in the water, this gives rise to greater concern than does rusty water 17].

The skeleton in animals is one of the most affected by manganese deficiency. In chicken the skeletal disorder perosis or "slipped tendon disease" results, in rats a condition known as chondrodystrophy, a type 7 skeletal disproportionate growth is observed [18]. When deficiency is imposed during prenatal period, the offsprings show congenital irreversible ataxia, characterized by lack of equilibrium, abnormal body reflexes and retractions of the head [19]. The same abnormal behaviour shown by offspring of manganese deficiency animals is also seen in a genetic mutant, the pallid mouse. In this strain the inability of the animal to swim, as well as the abnormal development of the otoliths, can be completely prevented by giving pregnant females a diet supplemented with manganese [20]. Manganese deficiency also affects brain function, this has been shown in that manganese deficient rats are much more susceptible to convulsion than are normal rats [20]. Ultra-structural defects were also observed in mice whose mitochondria showed evidence of membrane defects, the outer membrane was damaged and in some cases appeared to be missing [21].

5.7 Choice of analytical method

Various techniques are employed to determine manganese. These techniques include AAS, colorimetry, XRF spectrometry, ICP-AES, stripping voltammetry and HPLC [22]. Although these techniques deliver accurate results with some having low detection limits, the apparatus are expensive and not suitable for on-site, on-line routine analysis. Furthermore these techniques usually require labourious sample preparation using large sample volumes and involve complicated procedures which are time consuming. Spectrophotometric methods coupled with flow injection analysis proved to be a better alternative, but due to its high sample and reagent consumption, were ruled out in favour of the sequential injection system. In papers by Bowie *et al.* [22] and Gaikwad *et al.* [23] flow-injection analysis (FIA) is used with chemiluminescence (CL) mode of detection. However, in a paper by van Staden and Kluever [8] and a very recent paper by Kargosha and Noroozifar [9], FIA is used with a spectrophotometer as a mode of detection. Among the advantages of using flow-injection over other manual techniques [22] is a decrease in the amount of sample handling accompanied by the minimum of sample preparation steps.

Homogeneous reactions with sample and reagent both in the liquid phase are used in most of the FIA manifolds [24-26]. This set-up may provide some disadvantages, particularly if the reagent is expensive, slightly soluble or only available in the solid form. In fact one of the disadvantages of FIA is the relatively high reagent consumption per analysis.

The use of solid-phase reactors incorporated into FIA manifolds may offer certain advantages

over homogeneous systems [8, 27-30]. Reagent consumption is greatly decreased and the system is simplified with fewer junction for mixing of reagent, sample and carrier streams.

Sequential injection analysis (SIA), launched in 1990 [31, 32] is a technique that has a tremendous potential especially for on-line process measurements and in the monitoring of the environment, due to the simplicity and convenience with witch sample manipulations can be automated. The versatility of the technique is centred around a selection valve where each port of the valve allows a different operation to be performed [31-33]. The basic components of the system are a peristaltic pump with only one carrier stream, a single selection valve, a single channel and a detector. The concept is based on the sequential injection of a wash solution, sample zone and reaction zone(s) into a channel [34-37]. In this way a stack of well-defined zones adjacent to each other is obtained in a holding coil. After the valve has been selected to the detector position, the flow in the carrier stream is reversed and the zones mutually disperse and penetrate each other as they pass through a reaction coil to the detector. The flow reversal as a result of the injection step therefore creates a composite zone in which the sample and reagent zone penetrate each other due to combined axial and radial dispersion.

Some of the prerequisites needed for an analyser in the determination of manganese (II) in natural and effluents streams were that the system should be simple and robust, reliable with low frequency of maintenance and that the consumption of reagents should be very low. Sequential injection analysis seemed to be an ideal technique for such an analyser and this Chapter reports on a solid-phase reactor incorporated into a sequential injection analysis (SIA) system for the determination of manganese (II).

5.8 Manganese determination

Manganese (II) from a sample is oxidised by solid PbO_2 , embedded in silica gel beads, to produce the permanganate ion which is determined spectrophotometrically [38] at 526 nm.

5.8.1 Experimental

5.8.1.1 Reagents and solutions

All reagents were prepared from analytical-reagent grade chemicals unless specified otherwise. All aqueous solutions were prepared with doubly distilled water.

5.8.1.1.1 Stock manganese solution

A stock manganese (II) solution containing 1000 mg/ℓ Mn^{2+} was prepared by dissolving 3.639 g of manganese (II) chloride tetrahydrate (Merck, pro analysis) and diluting to 1ℓ with water. Working manganese (II) solutions in the range 0.1 to 7 mg/ℓ were prepared by appropriate dilution of the stock solution with 0.1 mol/ℓ HNO_3.

5.8.1.1.2 HNO_3 solution

A 0.5 mol/ℓ HNO_3 solution was prepared by dilution of 195 mℓ HNO_3 (55%), UNIVAR; SAARCHEM) with de-ionised water to 5 ℓ. The solution for the carrier stream was prepared by

appropriate dilution of this solution.

5.8.1.2 Instrumentation

The sequential injection system depicted in Fig 5.1 was constructed from the following components: a Gilson minipuls peristaltic pump (Model M312, Gilson, Villiers-le Bel, France); a 10-port electrically actuated selection valve (Model ECSD1OP; Valco Instruments, Houston, Texas); and a Unicam 8625 UV-Visible spectrophotometer equipped with a 10-mm Helma-type (Helma GmbH and Co., Mulheim/Baden, Germany) flow-through cell (volume 80 $\mu\ell$) for absorbance measurements.

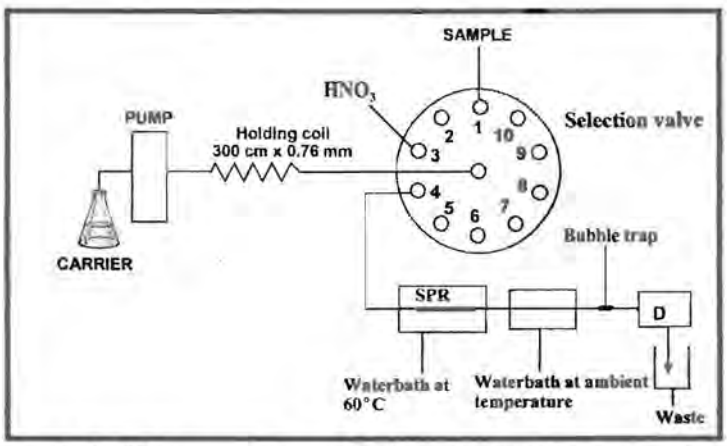

Fig. 5.1 A SIA system diagram for determination of manganese in water

Data acquisition and device control was achieved using a PC30-B interface board (Eagle Electric, Cape Town) and an assembled distribution board (Mintek, Randburg). The FlowTEK [38] software package (obtainable from Mintek) for computer-aided flow analysis was used

throughout for device control and data acquisition. All data given (mean peak height values) are the average of 10 replications.

5.8.1.3 The solid-phase reactor

The solid-phase reactor (SPR) was constructed using PTFE tubing with an internal diameter of 1.52 mm (Fig. 5.2). The reactor packing consisted of lead (IV)dioxide suspended on silica gel beads (35-70 mesh, 40 Å; Aldrich-Cemical Co. Gillngham-Dorset). The lead (IV) doxide was prepared as described by Rüter and Neidhart [29], the only difference being the use of commercial sodium hypochlorite (3.5% m/v when packed) for supplying the sodium hypochlorite. The bleach was added drop-wise to a solution of 150 g lead(II) acetate in 500 mℓ water in which 75 g of the previously mentioned silica gel was suspended with fast stirring. The bleach was added until precipitation of the lead (IV) dioxide was complete. The NaOCl oxidizes divalent lead to lead oxide according to the equation :

$$Pb(CH_3COO)_2 + NaOCl \rightarrow PbO_2 + 2CH_3COOH + NaCl$$

The mixture was then stirred for a further 60 minutes, vacuum-filtered, washed successively with dilute nitric acid and de-ionised water and the formed lead(IV) dioxide dried in a dessicator. The packing of each reactor was done by attaching the Teflon tube to a vibrating shaker after plugging the bottom end with glass wool. The prepared packing was then introduced via a funnel.

After packing each reactor had to be conditioned (run in) for at least 60 minutes before use.

Conditioning involved pumping de-ionised water through the reactor at a flow rate of 2.2 mℓ/min for 45 minutes and then the carrier for 15 minutes at the same rate. This was to ensure that there were no air pockets and to ensure close packing of the beads.

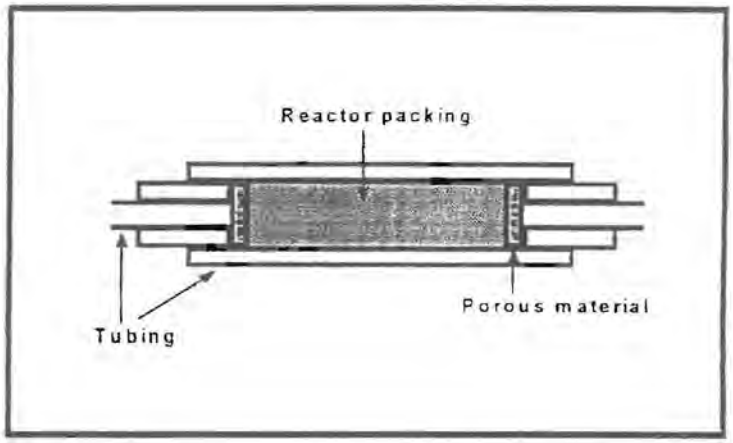

Fig. 5.2 Design of a tubular packed reactor

The lifetime of each reactor was established by comparing peak heights for the same standards from day to day. When the peak heights started to decrease systematically and drastically, the reactor had to be replaced. Another indication that the reactor was losing its oxidation capacity was the colour of the packing itself. At the beginning of a new conditioned reactor the colour of the packing was dark brown which gave a greyish appearance inside the PTFE tubing. After the reactor was in use for several samples (500-600) experiments and depending on the concentration of the manganese in the samples the colour of the packing at the front end of the reactor started to disappear. This meant that all of the PbO_2 had been stripped off the beads.

5.8.1.4 Procedure

A schematic diagram for the sequential injection analysis system in shown in Fig 5.1. The whole procedure, from sample injection to data processing and storage was computer controlled via the FlowTEK-program [38] except the water bath which had to be controlled manually. The whole procedure involved designing a method which allows a single cycle of the experiment to be run Fig 5.3 and Table 5.1 shows the device sequence analysis for one cycle.

The equation for this reaction is:

$$2Mn^{2+} + 5PbO_2 + 4H^+ \Rightarrow 2MnO_4^- + 5Pb^{2+} + 2H_2O$$

The reaction is thus pH dependent and the oxidation of Mn^{2+} is accompanied by a rise in the pH of the solution which results in a decrease in the efficiency of the reaction. The reaction conditions are kept at optimum by using an acidic carrier stream. After being placed in the carrier stream, the sample zone was pumped through the solid-phase reactor, which was immersed in the temperature controlled water bath.

For this study the determination of manganese was chosen. Mn^{2+}-ions in the sample zone was oxidised to MnO_4^- in the solid-phase reactor and the permanganate zone was channelled through a cooling system and then to a spectrophotometer for measurements at 526 nm. The decision to take measurements at this wavelength was based on a scan of the specified solution over the 200 to 1100 nm range.. The data obtained was converted to a response time graph illustrated on the computer screen as a peak profile. The maximum peak height was automatically

sequential injection system depends on the efficiency of the redox reaction at the inter-face between the solid and liquid phases of SPR. In addition to reactor packing, the reactor length and temperature had major effects and had to be optimized.

5.8.2.1.1 Reactor length

The response and precision of the system were studied by varying the reactor length between 8 and 16 cm (8, 10, 12, 14 and 16cm) with internal diameter fixed at 1.52 mm. A 7 mg/ℓ manganese (II) standard solution was used to optimized the system and the results are shown on Table 5.2. The internal diameter (i.d) of the SPR was kept constant at 1.52 mm because, i.d's smaller than that caused a dramatic deterioration in precision and also cause back pressure, while i.d's larger than 1.52 mm cause the response to drop, hence larger dispersion [8].

TABLE 5.2 Optimisation of reactor length

Reactor length (cm)	Peak height	%RSD
8	0.328	1.3
10	0.318	1.0
12	0.329	3.8
14	0.296	6.4
16	0.314	4.0

From results obtained it was concluded that with a longer reactor all the manganese was oxidized compared to the shorter reactor length. However, the 10 cm reactor length was found to be the ideal one for this type of analysis and was chosen as the optimum. It gave the best precision,

complete oxidation as well as a sharp peak compared to the longer reactors which gave a broad peak, but lower precision. Fig. 5.4 shows the responses and precision of this optimization.

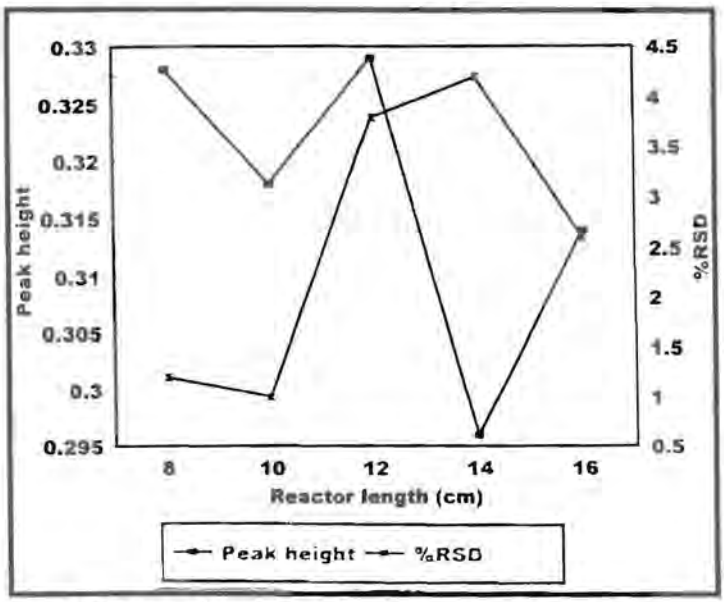

Fig. 5.4 Effect of reactor length on response and precision

5.8.2.1.2 Reactor temperature

The reactor temperature was varied between 60°C and 80°C with optimum results being obtained at 60°C. This confirmed the work done by van Staden and Kluever [8]. The response decreases with increase in temperature due to a faster reaction, and the reproducibility also showed a substantial decrease. Table 5.3 shows the results obtained and Fig. 5.5 the response and precision of this optimization.

TABLE 5.3 Optimization of reactor temperature

Temperature (°C)	Peak height	% RSD
60	0.328	1.2
65	0.318	1.4
70	0.313	1.6
75	0.322	3.4
80	0.247	1.97

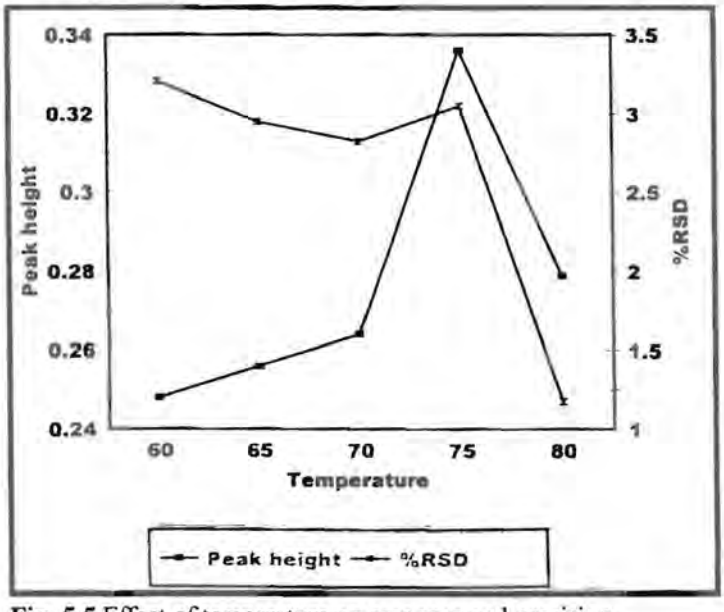

Fig. 5.5 Effect of temperature on response and precision

In the work done by Rüter and Neidhart [29], the highest possible temperature of 90 °C was used. Van Staden and Kluever [8] found this temperature to be unacceptable because of the high %RSD achieved at temperatures above 70°C as well as the problems experience with gas bubbles.

5.8.2.2 Chemical parameters

5.8.2.2.1 Acid concentration

As mentioned in the introduction, acidic conditions are required for the oxidation of Mn^{2+} ions to MnO_4^- ions. A manganese(II) concentration of 7 mg/ℓ was chosen as optimum. However, the choice of acid concentration in the carrier stream should give optimum performances without destruction of the SPR. Originally a problem was experienced with bubble formation when the carrier stream passed the heated reactor. This was at first attributed to a gas formed during the redox reaction, but it was later established that it was due to the carrier when heated. The problem was eventually solved by first bubbling nitrogen through the carrier and designing a glass tubing which trapped and eliminated the bubble before it could reach the detector. The bubble trap was 1 cm long with outlets of 0.76 mm internal diameter and a protrusion of 1 mm internal diameter where the bubble was trapped and destroyed (Fig 5.6).

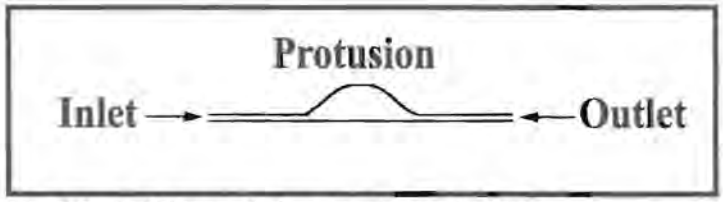

Fig. 5.6 Bubble trap designed to destroy bubbles

The bubble trap slowed down the flow rate because of that protrusion and hence the peak height was decreased by 5%. Table 5.4 shows the response with and without the bubble trap.

TABLE 5.4 Optimization of carrier concentration

(HNO_3) mol/ℓ	With bubble trap		Without bubble trap	
	Peak height	% RSD	Peak height	% RSD
0.05	0.308	3.8	0.3234	4.0
0.10	0.318	3.0	0.3349	3.9
0.15	0.312	1.4	0.3286	2.8
0.20	0.328	1.2	0.3444	2.0
0.25	0.312	1.4	0.3286	2.0

The effect of acid concentration between 0.05 mol/ℓ and 0.25 mol/ℓ was studied. The peak heights increased with increase in acid concentration, as was expected because the reaction is pH dependent. The precision improved between 0.10 and 0.25 mol/ℓ HNO_3 concentration. Below 0.1 mol/ℓ the precision was bad. At a concentration of 0.20 mol/ℓ the precision was 1.2%. Thus 0.20 mol/ℓ was therefore chosen as optimum concentration. This is a slight deviation from the work done by van Staden and Kluever [8] and Rüter and Neidhart [29] who both used 0.10 mol/ℓ as carrier concentration. Fig. 5.7 shows the response and precision of this optimisation.

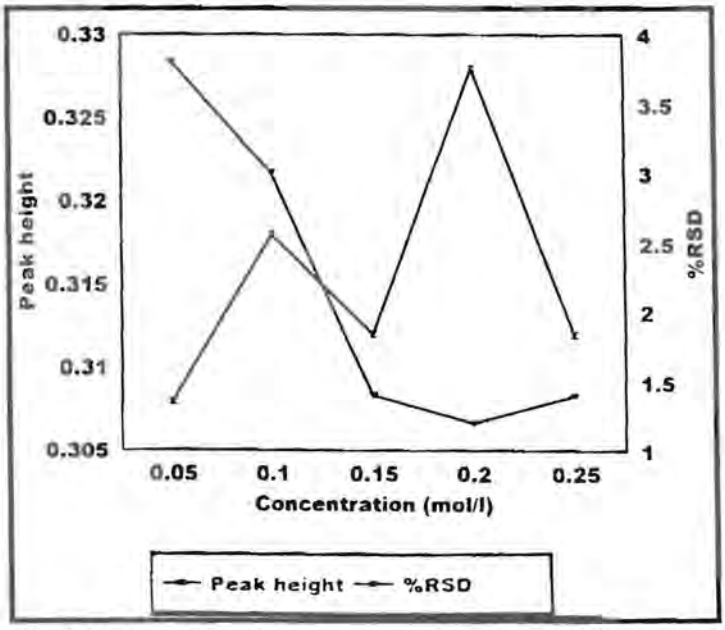

Fig. 5.7 Effect of concentration on response and precision

5.8.2.3 Physical parameters

5.8.2.3.1 Flow rate

The contact time between the sample zone containing manganese (II) and the solid phase reactor (SPR) is of utmost importance for the reaction to give the best analytical results. This period was influenced by the SPR parameters and by the flow rate. Flow rates between 0.9 mℓ/min and 2.5 mℓ/min were evaluated and Table 5.5 shows the results for this optimization.

TABLE 5.5 Optimization of flow rate

Rate (mℓ/ min)	Peak height	% RSD
0.9	0.292	3.8
1.3	0.282	1.5
1.7	0.308	2.7
2.2	0.325	1.2
2.5	0.328	1.7

The peak heights for higher flow rates were almost gaussian, with a small tailing effect due to fast rinsing of the SPR and a narrower longitudinal diffusion, but at the same time the peak heights increased substantially. The reason for this, is that at lower flow rates the manganese(II) took longer to flow through the SPR, producing a longer reaction time resulting in a higher yield of permanganate ions. The optimum flow rate was found to be 2.2 mℓ/min. The relative peak height was 0.33 at this flow rate with a 1.2% RSD. Fig. 5.8 shows the optimization of this flow rate.

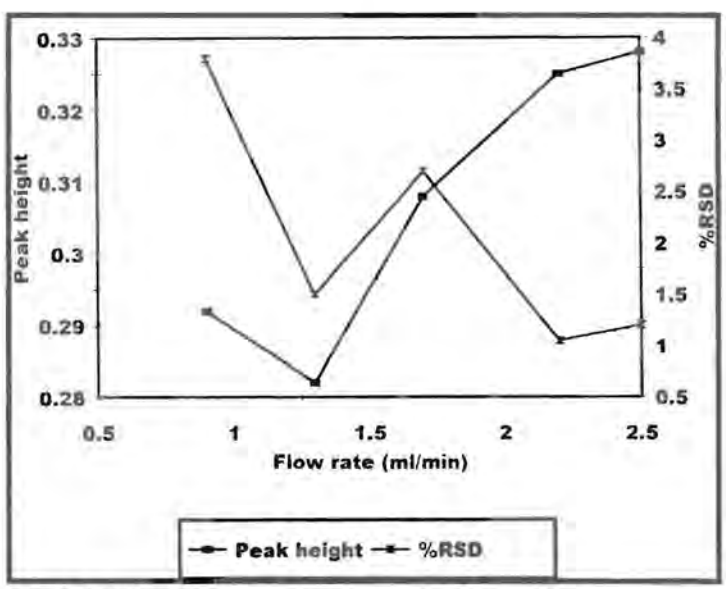

Fig. 5.8 Effect of flow rate on response and precision

5.8.2.3.2 Tube length

The tube length was optimised by distinguishing between the holding coil and the tube between the SPR and the detector. The holding coil was kept constant at a length of 3 m with an internal diameter of 0.76 mm. The tube length was varied between 20 and 60 cm with the internal diameter fixed at 0.76 mm. The optimum length of tubing between the SPR and the detector was 40 cm with a 1.1% RSD, which was the lower limit imposed by the system configuration. Table 5.6 shows the results for the optimization of this tube and Fig. 5.9 shows the response and precision of this optimization.

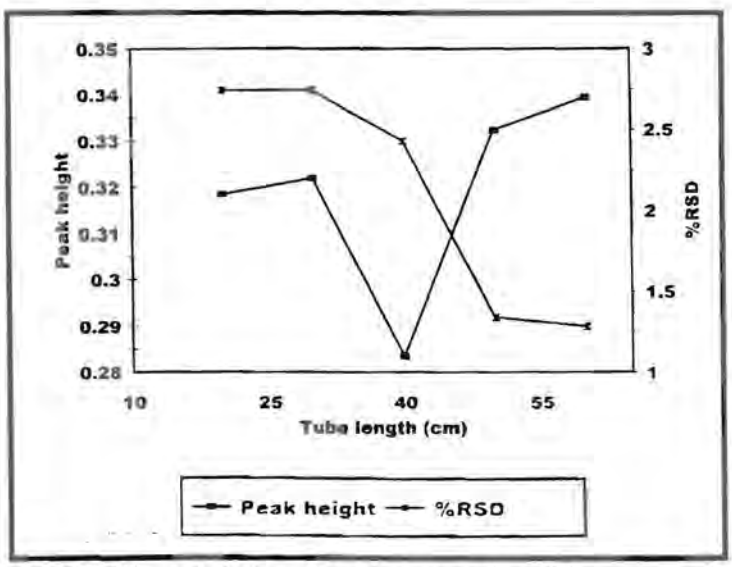

Fig. 5.9 Effect of tube length on response and precision

TABLE 5.6 Optimization of tube length

Tube length (cm)	Peak height	% RSD
20	0.341	2.1
30	0.341	2.2
40	0.330	1.1
50	0.292	2.5
60	0.290	2.7

5.8.2.3.3 Sample volume

The effect of sample volume was evaluated between 60 µℓ and 100 µℓ. Table 5.7 shows the results obtained for this optimization. The peak height increased with increase in volume of the sample, however the precision decreased as well. A value of 80 µℓ was chosen as optimum because it gave by the lowest %RSD of 1.04. Fig. 5.10 shows the response and precision of this optimization.

TABLE 5.7 Optimization of sample volume

Sample volume (µℓ)	Peak height	% RSD
60	0.268	1.2
70	0.273	1.4
80	0.328	1.2
90	0.288	2.3
100	0.338	4.3

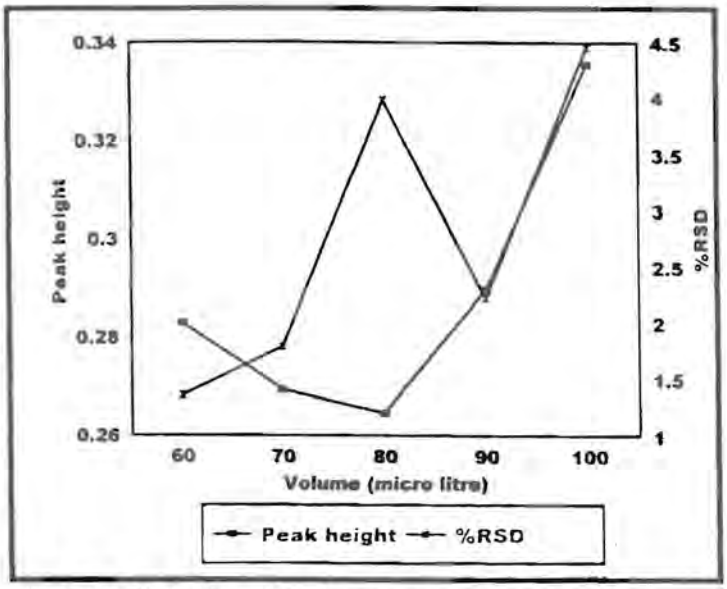

Fig. 5.10 Effect of sample volume on response and precision

5.8.3 Method evaluation

The system was evaluated with regard to linear range, accuracy, precision, detection limit, sample interaction (carry-over), interference, sampling rate and general problems experienced. The optimum conditions used are given in Table 5.8.

TABLE 5.8 Optimum (conditions) parameters

Parameter	**Optimum value**
Reactor length	10 cm
Reactor diameter	1.52 mm
Acid concentration	0.20 mol/ℓ
Flow rate	2.2 mℓ/min
Sample volume	80 µℓ
Tube length	40 cm
Tube diameter	0.76 mm

5.8.3.1 Linearity

The linearity of the SIA system was evaluated for analyte concentration ranging from 1 to 50 mg/ℓ under optimum conditions. The response was found to be linear in the range 1 to 7 mg/ℓ. Fig. 5.11 shows the calibration graph, the linear equation as well as the correlation co-efficient. The relationship obtained between response and concentration is given by the equation:

$$H = 0.01889x + 0.193 \ (r = 0.999, n = 7)$$

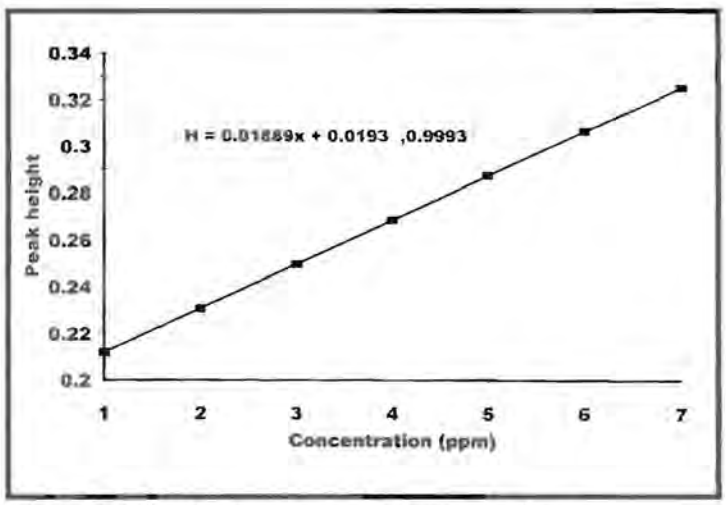

Fig. 5.11 Calibration graph using optimum conditions

where H is the relative peak height and x the analyte concentration (mg/ℓ). Real samples (water for domestic use and effluent streams) were analysed by the proposed SIA system. The results obtained are a mean of 10 repetitive analyses of each sample. Tables 5.9 and 5.10 shows the results obtained with the proposed system and the standard (ICP) method.

TABLE 5.9 Manganese in domestic water samples using SIA and ICP methods*.

Sample	Concentration of Mn in mg/ℓ		Relative standard deviation (%)	
	SIA	ICP	SIA	ICP
A	1.500	1.504	2.9	6.3
B	1.500	1.010	2.6	6.2
C	2.100	2.110	2.7	6.3
D	1.20	1.204	3.0	6.0
E	2.500	2.510	2.8	6.2

*n=10

TABLE 5.10 Manganese in effluent streams using SIA and ICP methods*.

Sample	Concentration of Mn in mg/ℓ		Relative standard deviation (%)	
	SIA	ICP	SIA	ICP
1	12.370	12.440	2.0	1.4
2	5.000	5.010	2.7	6.3
3	5.500	5.510	2.9	6.2
4	5.200	5.220	2.5	6.1
5	5.300	5.330	2.7	6.2

*n=10

5.8.3.2 Accuracy

The accuracy was evaluated by comparing results obtained with those from the standard (ICP) method. The results compared well (Tables 5.9 and 5.10). Since the majority of the tap water samples could only give a response in the SIA procedure after spiking, the accuracy of the method was also determined from these results using the method of standard addition.

5.8.3.3 Recovery

Real tap water samples which were found to contain no manganese at all were spiked with a 5 mg/ℓ standard manganese (II) solution to evaluate the recovery of the system. The formula used is:

$$\%\ Recovery = \frac{obtained}{\exp ected} x100\%$$

The expected concentration of manganese(II) for effluent streams spiked with 5.00 mg/ℓ Mn(II) standard solution was calculated with the calibration curve. The sample was analysed and the concentration (4.75 mg/ℓ) was compared with the expected concentration as shown above. The recovery ranged between 96.86 to 103.35 %.

5.8.3.4 Precision

The precision of the method was determined by 10 repetitive analyses of real sample solutions (Tables 5.9 and 5.10) as well as 10 repetitive analyses of standard solutions ranging from 1 to 7 mg/ℓ (calibtration graph, Fig 5.11). All these were carried out under optimum conditions. The % RSD for the standard solution was less than 1.8% and for real samples less than 2.9%.

5.8.3.5 Sample inter-action

The sample inter-action or carry-over was calculated according to the following formula:

$$\text{Interaction} = \frac{A_3 - A_1}{A_2} \text{ x } 100$$

$$\text{Interaction} = \frac{A_3 - A_1}{A_2} \times 100$$

where A_1 = peak height for sample without interaction

A_2 = peak height for sample with ten times the concentration of A_1

A_3 = peak height for interacted sample with the same concentration as A_1

In this study, A_1 was obtained with a 7 mg/ℓ manganese(II) standard solution and A_2 with a 70 mg/ℓ manganese(II) standard solution. A_3 was obtained by running in A_1 after having run in A_2. The values for A_1 and A_3 were 0.325 and 0.385 respectively. The value for A_2 was 6.12 giving an interaction value of 0.98% at a sampling rate of 50 samples per hour.

5.8.3.6 Detection limit

The detection limit was calculated using the formula:

$$DL = \frac{[(3\sigma + K) - C]}{m}$$

where $\sigma = 0.0016$ is the standard deviation of the baseline,

$K = (0.20)$ average signal value of the baseline

$C = 0.193$, which is the intercept of the calibration graph

$m = 0.01889$, which is the slope of the calibration graph.

The calculated detection limit was found to be 0.62 mg/ℓ.

5.8.3.7 Interferences

According to the work done by Rűter and Neidhart [30] only interferences for the determination of permanganate at 520 mm are reducing substances and coloured metal ions (iron(III), nickel(II), vanadium(V), copper(II), cobalt(II)) in high concentration as well as anions (halides, sulphate, phosphate, carbonate, acetate, thiocyanate, oxalate, sulphite).

In this determination at 526 nm the only ion found to be present in detectable amounts was iron (Fe) in the range 0.286 - 0.835 mg/ℓ. This did not cause any interference as the interference or tolerance level was found at 5 mg/ℓ. Finally the amount of manganese in the household water collected was found to contain very little amounts of manganese.

5.8.3.8 Sampling rate

The time taken for samples with low concentrations is 50 seconds per sample. The increased time is due to longer return-to-baseline times, implying longer washing-out times for flow cell. Thus a range of sampling rates are obtained varying between 50 and 72 samples per hour, depending on the manganese(II) concentration.

5.8.3.9 General problems

As was mentioned in subsection 5.8.2.2.1, the biggest problem encountered with this system was the bubbles that formed when the carrier passed through the water-bath. As mentioned the problem could be overcome by bubbling nitrogen through the carrier and placing a bubble trap between the detector and the water-bath (at ambient temperature).

Another problem was leaving the packed reactor in the laboratory exposed to the atmosphere. It was found that the response deteriorated compared to a freshly packed reactor. This problem was solved by storing the packed reactors in a dessicator until use.

5.9 Statistical comparison of techniques used

The statistical comparison was done between the SIA and ICP (standard method) to establish whether the proposed SIA method can be accepted as giving reliable results in manganese determination. The null hypothesis was used [40, 41]. For the null hypothesis, Ho we assert that the two methods agree, that is, the population mean difference is zero, H_o: $\mu_d = 0$. For the alternative hypothesis H_t:$\mu_d \neq 0$, where μ_d is the population paired by difference. The t-test with multiple samples (paired by difference) was applied to examine whether the two methods differed significantly at 95% level. The test is two tailed, as we are interested in both $\mu_d<0$ and $\mu_d>0$.

The mean, $\bar{x}_d$ standard deviation, S_d and $t_{calculated}$, $t_{calc.}$ are determined from the following equations:

$$\bar{x}_d = \frac{\sum x_d}{N}$$

$$S_d = \sqrt{\frac{\sum (x_d - \bar{x}_d)^2}{N-1}}$$

and

$$t_{calc.} = |\bar{x}_d| x \frac{\sqrt{n}}{s_d}$$

Table 5.11 gives the mean differences between SIA and ICP results for domestic water.

TABLE 5.11 Differences between SIA and ICP results for domestic water

Sample	x_{di}	$x_{di}^2 \times 10^{-4}$
A	0.004	0.16
B	0.010	1.0
C	0.010	1.0
D	0.004	0.16
E	0.010	1.

From Table 5.11 the following is deduced:

$$\sum x_{d1} = 0.038$$

and

$$\sum x_{d1}^2 = 3.32 \times 10^{-4}$$

Substituting for the mean and standard deviation with N = 5, we obtain:

$$\bar{x}_{d1} = 0.0076$$

and

$$S_{d1} = 0.0068$$

Table 5.12 gives the mean differences between SIA and ICP results for for effluent streams

TABLE 5.12 Differences between SIA and ICP results for effluent streams.

Sample	x_{d2}	x_{d2}^2
1	0.07	0.0049
2	0.01	0.0001
3	0.01	0.0001
4	0.02	0.0004
5	0.03	0.0009

From Table 5.12 the following is deduced:

$$\Sigma x_{d2} = 0.014 \qquad \text{and} \qquad \Sigma x_{d2}^2 = 0.0064$$

Substituting for the mean and standard deviation with N = 5, we obtain:

$$\bar{x}_{d2} = 0.0028$$

and

$$S_{d2} = 0.0397$$

From Table 5.11, $\bar{x}_{d1} = 0.0076, S_{d1} = 0.0068$ and $n = 5$.

Substituting for t_{calc} we find:

$$t_{calc} = 2.48$$

From Table 5.12, $\bar{x}_{d2} = 0.0028, S_{d2} = 0.0397$ and $n = 5$.

Substituting for t_{calc} we find:

$$t_{calc} = 0.1574$$

For both the determinations of manganese in tap water and effluent streams, there are five determinations, therefore $v = 4$. At 95% confidence level $t_{0.05,4}$ is 2.78. The critical t-values are therefore ±2.78. Since the calculated value is less than the critical value, the null hypothesis, H_0 cannot be rejected and it follows that at 95% of all samples drawn from the same population have a mean content within the acceptable range or only 5% of such samples fall outside the acceptable range. Hence it may be concluded that there is no significant statistical difference between the SIA and ICP techniques.

5.10 Conclusions

Mn determination by SIA with a solid-phase reactor incorporated into the SIA manifold is an improvement on the FIA system. In contrast to FIA, SIA once designed, does not need to be

physically reconfigured, even if essential parameters such as flow rates, sample and reagent volumes, reactant ratios and reaction times are to be altered. The system is easier to use and has the advantage of material saving. The system was found to be suitable for manganese determination in tap and domestic waters and effluent streams with a relative standard deviation of better than 3%.

5.11 References

1. F. A. Cotton and G. Wilkinson, **Advanced Inorganic Chemistry-A Comprehensive text,** Wiley & sons, New York, 1980.
2. J. V. Quagliano and L. M. Vallarino, **Chemistry 3rd ed.,** Prentice Hall, New Jersey, 1969.
3. E. Griffen and J. Am, **Water works Assoc., 52** (1960) 1326.
4. D.A. Crerar, R..K. Cormick, H. L. Barney. **General problems:** ***Geology and Geochemistry of Manganese,*** Ed by J. Varentsov and G. Grasselly; Springler verslag, Stuttgort, Germany, 1980.
5. W. Stumm, **Chemical processes lakes,** Wiley& sons, New York, 1985.
6. J. J. Delfino and G. F. Lee, **Environ. Sci. Technol. 2.,** (1968) 1094.
7. W. Balzer, **Geochim. Cosmochim. Acta, 46** (1982) 1153.
8. J. F. van Staden and L. G. Kluever, **Anal. Chim. Acta, 350** (1997)15.
9. K. Kargosha and M. Noroozifar, **Anal. Chim. Acta, 413** (2000) 57.
10. W. L. Masterdom, E. J. Slowinski and C. L Stanitski, **Chemical Principles with qualitative analysis,** Saunders, U.S.A, 1986.
11. A. Tulinsky and B. M. L Chen, **J. Am. Chem. Soc., 199** (1977) 3647.
12. C. E. Bomberger and D. M. Richardson, **J. Inorg. Nucl. Chem., 39** (1977)151.
13. C. Kies, **Nutritional Bio-availability of Manganese:** ***ACS Symposichem. Series 354, Am. Chem. SCC.,*** Washington, 1987.
14. J. Hauck, **Inorg. Nuch. Chem. Lett., 12** (1976) 893.
15. M. W. Coleman and L. T. Taylor, **Inorg. Chem., 16** (1977) 1114.
16. L. J. Boucher, **Co-ord. Chem. Rev., 7** (1972) 289.

17. A. H. Goodman, **Potable water Quality:** ***Developments in water treatment-2,*** Ed. by W. M. Lewis, Applied Science, London, 1980.

18. H. H. Sandstead, **J. Lab. Clin. Med., 98** (1981) 457.

19. G. K. Davis, **Ann. New York Alad. Sci., 355** (1980)130.

20. A. Wise, **Nutr. Abstr. Rev., Ser. A, 50** (1980) 319.

21. W. G. Pond, E. F. Walker jr., D. Kirkland, **J. Anim. Sci., 41** (1975) 1053.

22. A. R. Bowie, P. R. Fielden, R. D. Lowe and R. D. Snook, **Analyst, 120** (1995) 2119.

23. A. Gaikwad, M. Silva and D. Perez-Benditio, **Anal. Chim. Acta, 302** (1995) 275.

24. J. Ružička, E. H. Hansen, **Flow Injection Analysis, 2nd ed.,** Wiley & sons, New York, 1988.

25. Valcarsel, M. D. Luque de Castro, **Flow Injection Analysis. Principles and Applications,** Horwood, Chichester, 1987.

26. J. L. Burguera, **Flow Injection Atomic Spectrometry,** Marcel Dekker, New York, 1987.

27. M. D. Luque de Castro, **Trends Anal. Chem., 11** (1992)149.

28. J. Martinez Calatayud and J. V. Garcia Mateo, **Trends Anal. Chem., 12** (1993) 428.

29. J. F. van Staden and L. G. Kluever, **Anal. Chim. Acta, 369** (1998) 157.

30. J. Rűter and B. Neidhart, **Microchim. Acta., 18** (1984) 271.

31. J. Ružička and G. D. Marshall, **Anal. Chim. Acta, 237** (1990) 329.

32. J. Ružička, G. D. Marshall amd G. D. Christian, **Anal. Chem., 62** (1990) 1861.

33. G. D. Marshall, **Sequential-Injection Analysis,** PhD-thesis, University of Pretoria, 1994.

34. J. Ružička and T. Gűbeli, **Anal. Chem., 63** (1991) 1680.

35. T. Gűbeli, G. D. Christian and J. Ružička, **Anal. Chem., 63** (1991) 2407.

36. D. J. Tucker, B. Toivola, C. H. Pollema, J. Ružička and G. D. Christian, **Analyst, 119**

(1994) 975.

37. G. D. Marshall and J. F. van Staden, **Process Control and Quality, 3** (1992) 251.

38. E. B. Naidoo and J. F. van Staden, **Fresenius J. Anal. Chem., 370 (6)** (2001) 776.

39. G. D. Marshall and J. F. van Staden, **Analytical Instrumentation, 20** (1992) 79.

40. D. McCormick and A. Roach, **Analytical Chemistry by open learning. Measurement, Statistic and Computation.** Wiley and sons, Chichester, 1995.

41. D. A. Skoog, D. M. West and F. J. Holler, **Fundamentals of Analytical Chemistry, 7th ed.** Saunders, USA,. 1996.